

METHOD FOR THE NON-INVASIVE MEASUREMENT OF THE FETAL
ELECTROCARDIOGRAM

SERGIO TASCÓN MORALES



UNIVERSIDAD DEL VALLE
FACULTAD DE INGENIERÍA
ESCUELA DE INGENIERÍA ELÉCTRICA Y ELECTRÓNICA
SANTIAGO DE CALI, COLOMBIA
2017

METHOD FOR THE NON-INVASIVE MEASUREMENT OF THE FETAL
ELECTROCARDIOGRAM

SERGIO TASCÓN MORALES

Bachelor final project

Director:
Asfur Barandica, M.Sc.

Consultant:
Peter Husar, Ph.D.



UNIVERSIDAD DEL VALLE
FACULTAD DE INGENIERÍA
ESCUELA DE INGENIERÍA ELÉCTRICA Y ELECTRÓNICA
SANTIAGO DE CALI, COLOMBIA
2017

ACKNOWLEDGMENTS

I would first like to thank God for giving me big dreams, and for showing me the path that I should follow to reach them. For giving me everything I need, for guiding me, for conferring on me strength and faith.

Special thanks to my project director, Asfur Barandica, for giving me the opportunity of working on this fascinating topic. I would also like to thank professor Husar, for giving me his support and advice whenever I had a question, for being an academic role model.

Special thanks to my classmates, which I prefer to call friends. Thanks to Laura Riascos, Jose Arturo García, Sergio Andrés Castro, Sebastián Ramírez, Alejandro Tenorio, Ivan Góngora, Eduardo Osorio, William Giraldo and all the friends I had the opportunity of working and sharing with. I can say for sure that I learned something from everyone.

Finally, I must express my very profound gratitude to my parents, Stella Morales and Gustavo Tascón, and also to my sister and brother, Natalia and Juan Felipe, for providing me with unfailing support and continuous encouragement throughout my years of study and through the process of becoming who I am today. This accomplishment would not have been possible without them. My sincere thanks also goes to my aunts Neyla Morales and Sandra Tascón, for their important support. I thank my grandmother, Bertha Ligia, who is still today, from heaven, an inspiration for my life.

CONTENTS

INTRODUCTION	11
1 REFERENCE FRAMEWORK	13
1.1 THEORETICAL BACKGROUND	13
1.1.1 Basics of Bioelectrical Signals	13
1.1.2 Physiology and Anatomy of the Human Heart	15
1.1.3 Electrical Activity of the Human Heart	16
1.1.4 Electrocardiography	17
1.1.4.1 Electrocardiography in Adults and Children	19
1.1.4.2 Fetal Electrocardiography	21
1.1.5 Independent Component Analysis as Blind Source Separation Technique	24
1.1.5.1 Basic ICA Model	24
1.1.6 Adaptive Filters	25
1.1.6.1 Adaptive Noise Canceller	26
1.2 HISTORICAL FRAMEWORK	27
1.2.1 Review of Relevant Developments in Non-invasive fECG Extraction	27
1.2.2 Comparison Table	35
1.3 USED DATABASES	36
1.3.1 Abdominal and Direct Fetal Electrocardiogram Database	36
1.3.2 Non-Invasive Fetal Electrocardiogram Database	37
1.3.3 DaISy Database	38
2 METHODOLOGY	39
2.1 Review of Relevant Documentation	39
2.2 Design of the Algorithm	40
2.2.1 Pre-Processing Stage	40
2.2.1.1 Baseline Wander Removal	40
2.2.1.2 Powerline Interference Removal	45
2.2.2 Extraction Algorithm	45
2.2.2.1 First Approach - fECG Extraction Using Thoracic Signals	45
2.2.2.2 Second Approach - fECG Extraction Without Using Thoracic Signals	51
2.3 Evaluation of the Algorithm	53
2.3.1 Test Protocol and Metrics to Measure Effectiveness	53
2.3.1.1 Test Protocol	54
2.4 Comparison With Other Algorithms	56
2.4.1 Compared Methods	56
2.4.2 Comparison Test	56
3 RESULTS	57
3.1 Results of First Approach	57
3.1.1 First Approach - Results on the Non-Invasive Fetal Electrocardiogram Database	57

3.1.2	First Approach - Results on the DaISy Database	58
3.2	Results of Second Approach	60
3.2.1	Second Approach - Results on the Abdominal and Direct Fetal Electrocardiogram Database	60
3.2.2	Second Approach - Results on the Non-Invasive Fetal Electrocardiogram Database	63
3.2.3	Second Approach - Results on the DaISy Database	63
3.3	Comparison Test	64
3.3.1	Results of ICA	64
3.3.1.1	ICA - Results on the Abdominal and Direct Fetal Electrocardiogram Database	64
3.3.1.2	ICA - Results on the Non-Invasive Fetal Electrocardiogram Database	64
3.3.1.3	ICA - Results on the DaISy Database	64
3.3.2	Results of Adaptive Filter	66
3.3.2.1	Adaptive Filter - Results on the Non-Invasive Fetal Electrocardiogram Database	66
3.3.2.2	Adaptive Filter - Results on the DaISy Database	67
3.4	Analysis of Results	67
3.4.1	First Approach	67
3.4.2	Second Approach	69
3.4.3	Comparison	70
4	CONCLUSIONS AND FUTURE WORK	71
4.1	Conclusions	71
4.2	Future Work	73
5	BIBLIOGRAPHY	74

List of Figures

1	Cell under rest conditions	14
2	Typical action potential from a ventricular myocardial cell	14
3	Structure of the human heart and pathway of blood	16
4	Electrical conduction system of the heart	16
5	Different types of action potentials produced in the heart	18
6	Vectors associated to the heart in different moments of the cardiac cycle	19
7	Waves, segments and intervals of the ECG	20
8	Standard distribution of the electrodes for the measurement of the precordial leads	21
9	First recorded fECG	22
10	Fetal presentations	24
11	Different possible vertex positions	24
12	Structure of an adaptive filter	26
13	Structure of an Adaptive Noise Canceller	27
14	General scheme of the combined method proposed by Ye-Lin et al.	29
15	General scheme of the Multistage Interference and Noise Cancellation proposed by Fatemi et al.	31
16	General scheme of the wavelet-based method proposed by Raoof	33
17	General scheme of the adaptive filtering method proposed by Liu	34
18	Block diagram of the proposed methodology	39
19	Example of abdominal signal from Non-Invasive Fetal Electrocardiogram Database	41
20	Spectrum of the original signal from Non-Invasive Fetal Electrocardiogram Database	41
21	Result of FIR filter on abdominal signal	42
22	Estimated baseline through polynomial fitting	43
23	Result of polynomial fitting	43
24	Block diagram of the Pan-Tompkins algorithm	44
25	Example of erroneous estimation of baseline	44
26	Magnitude response of implemented notch FIR filter	45
27	Phase response of implemented notch FIR filter	46
28	First Proposed Approach - fECG Extraction Using Thoracic Signals	46
29	Basic structure of the implemented ANC	47
30	Basic structure of ICA Analysis block	48
31	Structure of the matched filter used for selection of best fetal component	50
32	Map of MATLAB functions and scripts for first approach	52
33	Second Proposed Approach - fECG Extraction Without Using Thoracic Signals	52
34	Map of MATLAB functions and scripts for second approach	53
35	Example of signal interval discarded due to measuring distortion	54
36	General steps for test protocol	54
37	Independent components after FastICA algorithm on Non-Invasive Fetal Electrocardiogram Database - First Approach	57
38	Abdominal signals after pre-processing stage on DaISy Database - First Approach	58
39	Signals after ANC on DaISy Database - First Approach	59

40	Independent components obtained with JADE algorithm on DaISy Database - First Approach	59
41	fECG signal obtained on DaISy Database - First Approach	60
42	fECG signals obtained on Abdominal and Direct Fetal Electrocardiogram Database (dataset r08) - Second Approach	61
43	fECG signals obtained on Abdominal and Direct Fetal Electrocardiogram Database (all datasets) - Second Approach	62
44	Output signal on Non-Invasive Fetal Electrocardiogram Database - Second Approach	63
45	fECG signal obtained on DaISy Database - Second Approach	64
46	Result of the JADE algorithm on the Abdominal and Direct Fetal Electrocardiogram Database	65
47	Result on the FastICA algorithm on the Non-Invasive Fetal Electrocardiogram Database	65
48	Result for the FastICA algorithm on the DaISy Database	66
49	Result for the ANC on the Non-Invasive Fetal Electrocardiogram Database	67
50	Result for the ANC on the DaISy Database	68
51	Most prominent signal from ANC on the DaISy Database	68

List of Tables

1	Comparison table of reviewed fECG extraction methods	35
2	Main characteristics of the Abdominal and Direct Fetal Electrocardiogram Database	36
3	Main characteristics of the Non-Invasive Fetal Electrocardiogram Database	37
4	Main characteristics of the DaISy Database	38
5	Selected data for the Abdominal and Direct Fetal Electrocardiogram Database	55
6	Comparison between R-peak locations and intervals on the Abdominal and Direct Fetal Electrocardiogram Database	62

ACRONYMS

<i>aECG</i>	Abdominal Electrocardiogram
<i>ANC</i>	Adaptive Noise Canceller
<i>ANFIS</i>	Adaptive Neuro Fuzzy Inference System
<i>ANN</i>	Artificial Neural Networks
<i>bpm</i>	Beats Per Minute
<i>BSS</i>	Blind Source Separation
<i>DEFL</i>	Denoising by Deflation
<i>ECG</i>	Electrocardiogram
<i>EKF</i>	Extended Kalman Filter
<i>EKS</i>	Extended Kalman Smoother
<i>EMD</i>	Empirical Mode Decomposition
<i>ESC</i>	Event Synchronous Canceller
<i>EVD</i>	Eigenvalue Decomposition
<i>fECG</i>	Fetal Electrocardiogram
<i>FFT</i>	Fast Fourier Transform
<i>fHR</i>	Fetal Heart Rate
<i>fHRV</i>	Fetal Heart Rate Variability
<i>FIR</i>	Finite Impulse Response
<i>HR</i>	Heart Rate
<i>IC</i>	Independent Component Analysis
<i>ICA</i>	Independent Component Analysis
<i>IIR</i>	Infinite Impulse Response
<i>LMS</i>	Least Mean Square
<i>LPC</i>	Linear Prediction Coding
<i>LTI</i>	Liner Time-Invariant
<i>LTV</i>	Linear Time-Variant
<i>mECG</i>	Maternal Electrocardiogram
<i>MINC</i>	Multistage Interference and Noise Cancellation
<i>MLS</i>	Minimum Least Square
<i>MRANC</i>	Multireference Adaptive Noise Canceller
<i>MSE</i>	Mean Square Error
<i>NLMS</i>	Normalized Least Mean Square
<i>PRD</i>	Percent Root-Mean Square Difference
<i>PSO</i>	Particle Swarm Optimization
<i>RLS</i>	Recursive Least Square
<i>RPG</i>	Relative Power Gain
<i>SNR</i>	Signal to Noise Ratio
<i>SVD</i>	Singular Value Decomposition
<i>SVR</i>	Singular Value Ratio
<i>UWT</i>	Undecimated Wavelet Transform
<i>WT</i>	Wavelet Transform

ABSTRACT

This document contains the information that corresponds to the development of an algorithm for the non-invasive extraction of the fetal electrocardiogram. The algorithm was implemented with a combination of Independent Component Analysis (ICA) and adaptive filters. Two approaches are proposed: The first approach uses both thoracic and abdominal signals and the second one uses abdominal signals only. For testing the performance of the approaches three databases are used. Two of these databases contain both abdominal and thoracic signals and one of the databases contains abdominal signals among with a direct (invasive) measurement. The first approach was tested on the two databases that contain thoracic signals and results show a good performance for one of the databases, for which all fetal R-peaks can be properly identified and for which some presumable T and P waves can be observed. For the other database the very low SNR make it impossible to separate the fetal signal. The second approach was tested on the three databases. Results lead to the appropriate identification of most of the fetal R-peaks for two of the three databases.

Key words: Fetal electrocardiogram, non-invasive extraction, independent component analysis, adaptive filters.

RESUMEN

Este documento contiene la información correspondiente al desarrollo de un algoritmo para la extracción no invasiva del electrocardiograma fetal. El algoritmo fue implementado con una combinación de Análisis de Componente Independiente (ICA, por sus siglas en inglés) y filtros adaptativos. Dos enfoques son propuestas: El primero usa señales torácicas y abdominales, mientras que el segundo usa solamente señales abdominales. Para probar el rendimiento de los enfoques, tres bases de datos son usadas. Dos de las tres bases de datos contienen tanto señales abdominales como señales torácicas y una de las bases de datos contiene sólo señales abdominales junto con una medición directa (invasiva). El primer enfoque fue probado en las dos bases de datos que contienen señales torácicas y los resultados muestran un buen rendimiento para una de las bases de datos, para la cual todos los picos R fetales pueden ser apropiadamente identificados y para la cual algunas ondas T y P presumibles pueden ser observadas. Para la otra base de datos el muy bajo SNR hace imposible separar la señal fetal. El segundo enfoque fue probado en las tres bases de datos. Los resultados llevan a la apropiada identificación de la mayoría de los picos R fetales para dos de las tres bases de datos.

Palabras clave: Electrocardiograma fetal, extracción no invasiva, análisis de componente independiente, filtros adaptativos.

INTRODUCTION

Non-invasive fetal electrocardiogram (fECG) extraction consists on placing a determined number of electrodes on the abdomen of the pregnant woman in order to measure the voltage differences between them, and then extracting the fECG signal from the measured abdominal signal (called abdominal electrocardiogram - aECG). In this case, the aECG signal contains a mixture of different signals, which include the fECG, brain activity of the fetus, the maternal ECG (mECG) component, muscular and respiratory activity of the mother, power line interference, baseline wander and random electronic noise [1][2][3]. The existing time and frequency overlap between the mECG component and the fECG makes it impossible to use conventional filtering techniques to extract the fECG from the aECG [4]. The multiple layers of tissue that exist between the fetus and the measuring electrodes constitute a complex path for the signals that travel from the fetal heart to the surface of the mother's abdomen. Because of these interferences and because the fECG component has a very low Signal to Noise Ratio (SNR), the extraction of the fECG from the aECG becomes a hard task [1].

During pregnancy, monitoring the heart condition of the fetus becomes very important, because it allows to test the well-being and also brings the possibility of diagnosing diseases [5]. Changes in amplitudes and intervals of ECG waves are related with fetal distress. Also, hypoxia may produce changes on the waveform of one of the segments of the ECG [6]. This means that recovering the fECG waveform may bring possibilities for fetal cardiac diagnosis and thus for its treatment. Although the fECG can be recorded invasively by placing an electrode on the fetal scalp during labor [1], this invasive recording can be accomplished only at the last stage of pregnancy, after rupture of the membranes [7][8] and under limited clinical conditions, producing a risk, which is small, to the safety of the fetus [1]. With non-invasive measurement, the fECG can theoretically be recorded earlier during pregnancy and there is no associated risk [8][9].

Some developments have been made in the recent years in the field of non-invasive fECG extraction and different techniques have been implemented to extract the fECG from the aECG. These techniques are, among others, Wavelet transforms, Singular Value Decomposition, Independent Component Analysis (ICA), Artificial Neural Networks (ANN), Adaptive Neuro-Fuzzy Inference System (ANFIS). A review of some previously proposed approaches is presented in section 1.2. The review of the previous works is very important in order to understand how different methods can be applied to the problem, having each one different requirements and performances.

The general objective of this project is to design and implement an algorithm for the non-invasive extraction of the fetal electrocardiogram. Four specific objectives have been proposed for the project: (1) Study the state of the art of the non-invasive measurement of the fECG, (2) Develop an algorithm for the extraction of the fetal electrocardiogram, particularly the morphological characteristics, (3) Evaluate, using three different databases, the effectiveness of the designed algorithm for the adequate extraction of the fetal electrocardiogram. After evaluation, determine the scope and limitations of the designed algorithm, and (4) Compare the designed algorithm to other algorithms in order to evaluate its effectiveness in relation

with the appropriate extraction of the fECG.

This document is divided as follows: Section one contains the theoretical background, the historical framework and the description of the databases used for the development of the algorithm. The theoretical background provides the concepts that are required to understand the context of the problem. The historical framework presents a revision of relevant documents about different methods that have been proposed previously for the non-invasive extraction of the fECG, including a comparison table between them. Section two contains the methodology applied for solving the addressed problem. In section three are presented the results of the executed tests and their corresponding analysis. Section four provides the conclusions and future work.

1 REFERENCE FRAMEWORK

1.1 THEORETICAL BACKGROUND

In this section are presented the basic concepts that are required to fully understand the context of the developed method for the non-invasive extraction of the fECG and the different processes that are involved in the electrocardiography. At first, the genesis of the biosignals in the human body from the cellular perspective is presented. Then, the topics related to the human heart such as its physiology and its electrical activity are reviewed. After that, the electrocardiography is presented for both adults and fetuses, including the way in which the electrical signals of the heart are recorded non-invasively through electrodes placed on the body.

1.1.1 Basics of Bioelectrical Signals

Understanding the cellular genesis of biosignals is an important factor in the field of electrocardiography. This part of the document provides the basic concepts that should be considered in order to understand how the electrical activity of the heart is produced.

Every cell in the human body is a structure that has a bounding membrane which is basically formed by a number of lipid layers with low conductivity. Because of the permeability properties of the membrane, certain substances can move from the inside of the cell to the outside, using diverse specific channels (ion channels) that are opened and closed over time. This means that the membrane establishes a process in which some substances can pass through it, and some other substances are blocked [10][11]. These substances include sodium, potassium, calcium and chloride. A certain number of ions of the mentioned substances find a path through the mentioned channels. Because the channels are opening and closing over time, there is a variation in the membrane conductance, which produces, at the same time, an alteration in the membrane potential [11].

Under resting conditions, the membrane potential is negative since the concentration of negative ions is higher in the inside of the cell with respect to the outside (in the outside zero voltage is assumed). As mentioned before, the permeability of the cell allows some ions to pass across the membrane; this can change the concentrations of ions in the inside and the outside of the cell and, therefore, the permeability can influence the magnitude of the membrane potential. The resting conditions of the cell are illustrated in Figure 1, for which it has been assumed that potassium ions are inside the cell and sodium ions are outside. The normal range for the resting membrane potential is -60 to -100 mV, but this may change depending on the type of cell [10].

As stated before, the permeability of the membrane makes possible that some ions can pass across it. When there are rapid alterations in the membrane permeability, a change in the membrane potential is produced and an action potential is generated [10]. In this way, action potentials are fast variations in the membrane potential. Normally, action potentials begin with an abrupt change from the resting potential (which is negative) to a positive potential.

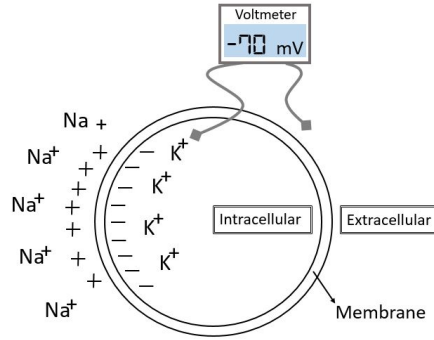


Figure 1: Cell under resting conditions (based on [12])

After the maximum value is reached, the action potential has a rapid decrease and reaches again the negative resting potential [13]. Figure 2 shows a typical action potential from a ventricular myocardial cell.

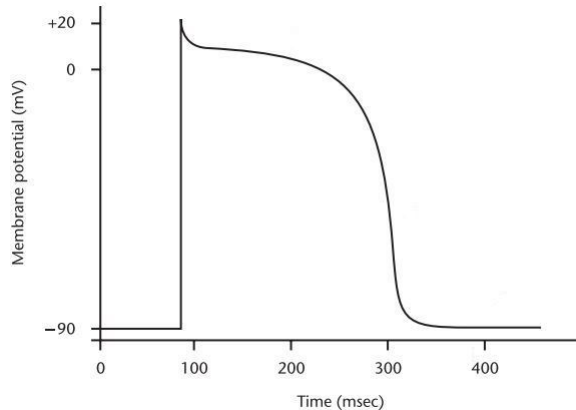


Figure 2: Typical action potential from a ventricular myocardial cell (modified from [11])

The behaviour of the action potential shown in Figure 2 can be understood as a two-phases behaviour in which the first phase is called depolarization, which corresponds to the abrupt change in the membrane potential from the resting potential to a positive value, crossing the zero level (see Figure 2). The second phase is called repolarization and during this phase the potential returns to its resting level [10]. From Figure 2 it can be observed that the depolarization process is much faster than the repolarization process. Also, the repolarization has a particular waveform, which can be explained through the alterations in the ion channels, so that different types of ions (mainly potassium and calcium) travel, with different rates, from the outside of the cell to the inside or viceversa [11].

Until this point it has been explained that the permeability of the membrane and the difference of concentrations between the inside and the outside of the cell that the permeability causes produce a membrane potential that varies over time. However, the variation in the

membrane potential will only occur if some external stimulus perturbs the resting membrane potential. The stimulus can be, for instance, a current (a propagated action potential) that comes from another cell. Therefore, a first membrane depolarization activates a contiguous membrane so that a new action potential is generated, and this process is repeated for a number of cells, until the level of the generated action potential is not sufficient to activate an adjacent membrane. The membrane has, however, a limitation in its response to new stimulus, which is called “refractory” state. The refractory state is the condition of the membrane of not being able to immediately react to a new stimulus and this state is related to changes in the permeability of the membrane [10].

Before an action potential can propagate, it must be generated somewhere. In the case of the heart, the action potentials are generated by cells called *pacemakers*, which are cells that have the ability to suddenly depolarize [11]. Pacemakers are situated in different parts of the heart, as will be explained later.

1.1.2 Physiology and Anatomy of the Human Heart

The heart can be seen as a structure with two separate pumps, which are divided by a group of muscular tissue called septum [10]. The right pump makes blood flow through the peripheral organs, and the left pump is responsible for sending blood through the lungs [14]. Each pump contains two chambers, atrium and ventricle. The atrium is the chamber where the blood enters and the ventricle is the chamber where the blood leaves the heart. There are four valves in the heart that are responsible for defining the direction in which the blood flows. Each side of the heart possesses two valves: one located between the atrium and the ventricle and one controlling the entrance of blood to the atrium, i.e between the atrium and the arteries [10]. As shown in Figure 3, each valve has a specific name depending on the side of the heart in which it is located and depending on its primary function. This figure also shows the pathway of the blood in the heart.

The heart has a surrounding wall which is called myocardium, which is composed basically by muscle cells and specialized cells. The muscle part allows the heart to contract in order to pump the blood through the body [1][10]. The specialized cells establish a connection with the conduction system, so that electrical impulses can be spread through the heart. Once an electrical impulse is generated and spread, a cardiac cycle starts. The electrical impulse activates the contraction of the heart, which means the contraction occurs after the electrical event [10]. The contraction has a specific sequence, which starts with the contraction of the atria (atrial systole), continues with the contraction of the ventricles (ventricular systole), and ends with diastole, which is the relaxation of both atria and ventricles [15].

The sequence of the cardiac cycle can be explained as follows: the cycle starts at the right atrium where blood with low oxygen content is accumulated. Once the right atrium starts contracting, the collected blood is passed to the right ventricle, from where it is sent to the lungs. The lungs “clean” the blood by extracting carbon dioxide and introducing more oxygen. Oxygen-rich blood returns to the heart, but in this case the entrance is the left atrium. The contraction of the left atrium sends the oxygenated blood to the left ventricle. At this point the ventricle contains blood with high amount of oxygen and that blood must circulate

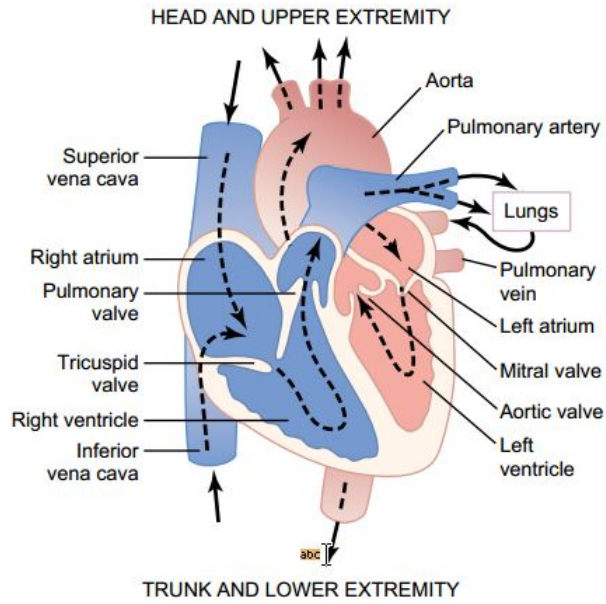


Figure 3: Structure of the human heart and pathway of blood (from [14])

through all organs and tissues (except the lungs), using the arterial vessels as conduits [10].

1.1.3 Electrical Activity of the Human Heart

As stated before, the electrical impulse is responsible for the activation of the cardiac cycle. The parts of the heart that constitute the conduction system are the sinoatrial node (SA node), the internodal atrial pathways, the atrioventricular node (AV node), the bundle of His and the Purkinje fibers [15]. Figure 4 shows the electrical conduction system of the heart.

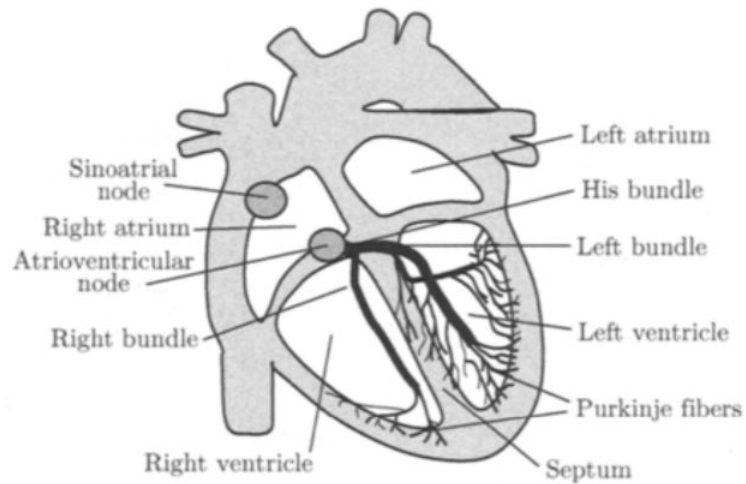


Figure 4: Electrical conduction system of the heart (from [10])

It has been explained that before an action potential can propagate, it must be originated by a pacemaker. Pacemakers are cells that suddenly depolarize. From the mentioned parts of the conduction system, the SA node is the element that depolarizes most rapidly. This node is therefore the default pacemaker and its rate of depolarization determines the heart rate [15]. The electrical impulse that is generated at the SA node propagates through the heart, allowing the mechanical activation (contraction) and relaxation of the atria and ventricles. The first event that takes place with the electrical impulse is the electrical activation of both atria. The electrical impulse travels until it reaches the AV node, where it is delayed. During the time in which the impulse is delayed at the AV node, the amount of blood in the ventricles increments. This occurs before the ventricular contraction takes place. The delay is due to the fact that the muscle cells of the AV node are not capable to conduct the impulse as fast as other muscle cells do. The impulse reaches then the bundle of His, which establishes the electrical connection between the AV node and the ventricles. At this point the ventricular contraction starts and the impulse continues spreading until it reaches the Purkinje fibers, which are specialized conduction fibers [10].

1.1.4 Electrocardiography

The property of the human body of being a volume conductor makes that fluctuations in potentials produced inside the body can be recorded extracellularly. This means that the action potentials (particularly their algebraic sum) produced in the heart can be perceived from the surface of the body. The measurement of the potential fluctuations that manifest the electrical activity of the heart is called ECG [15].

Different types of action potentials are produced in the heart, depending on the specific area where they are examined. Figure 5 shows that normally the part of the action potentials that corresponds to the depolarization phase is steeper than the part that corresponds to the repolarization phase, which tends to be rounded. As stated before, the signal that is recorded extracellularly is the algebraic sum of the action potentials [10]. This sum produces the typical ECG waveform, shown at the bottom of the figure.

The dipole model is generally used to understand how the waves of the ECG are generated. This model considers two components: the dipole itself, which is a representation of the electrical activity, and the geometry and electrical properties of the surrounding body. In terms of the electrical activity, for the propagation of an action potential through a cell there is an associated intracellular current whose direction is the same of the propagation, at the interface of tissue in resting and depolarization conditions. Because of the conservation of charge, there is also an equal extracellular current which flows in the opposite direction of the intracellular current [11]. For each group of cells concurrently depolarizing there is an equivalent dipole source representation and for each current dipole source a vector can be associated. The vector describes the main parameters of the dipole, such as time-varying position, orientation and magnitude. When all groups of cells are considered, it can be assumed that the associated vectors produce a “dominant” vector. This dominant vector represents the main direction of the electrical impulse [10]. Figure 6 allows a better understanding of what has been explained about the dipole and the vectors. The figure shows how the ECG typical wave (which will be reviewed in detail later) is produced according to the condition of the vectors that represent

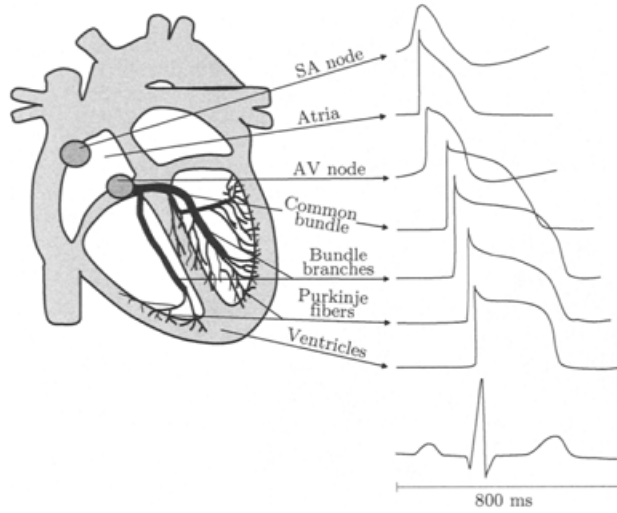


Figure 5: Different types of action potentials produced in the heart (from [10])

the electrical activity that is produced during the cardiac cycle. The signal is measured in this case by an electrode placed in the position indicated with the symbol \vdash . It can be noticed from the figure that the waves that correspond to the ventricular depolarization have a higher amplitude as compared to those of the atrial depolarization and ventricular repolarization. The reason for this is that the ventricles have a larger muscle mass. From the figure it can also be clearly observed that when the dominant vector points to the measuring electrode, the recorded signal tends to increase its magnitude. When the dominant vector is pointing to any other direction, the magnitude of the signal tends to decrease, reaching negative values in case the dominant vector is directed away from the measuring electrode [10].

The typical ECG signal is shown in Figure 7. Waves P, Q, R, S, T and U (named by Einthoven [11]) are marked. The group composed by the Q, R and S waves is referred to as QRS complex. At first, some elements should be specified in order to completely define the waveform and the parameters that play an important role in the analysis of the ECG: The isoelectric line is the horizontal line and it represents the time intervals during which there is no electrical activity reflected in the ECG; the segments are duration of the isoelectric line between subsequent waves; and the intervals are the time between same segments of contiguous waves [16]. Duration of the different waves is defined by the time moments at which the wave either changes notably with respect to the isoelectric line or crosses it [10].

As Figure 5 already suggested, the different waves of the typical ECG represent a special event that occurs at a particular part of the heart. The P-wave corresponds to the depolarization of the atria. Repolarization of the atria cannot be observed because it occurs simultaneously with the ventricular depolarization, which is reflected by the QRS complex. The T-wave represents the ventricular repolarization. Normally the U-wave appears only in one quarter of population. The origin of this wave is not completely understood but it has been suggested that it appears due to after-potentials generated by mechanical-electric feedback [16].

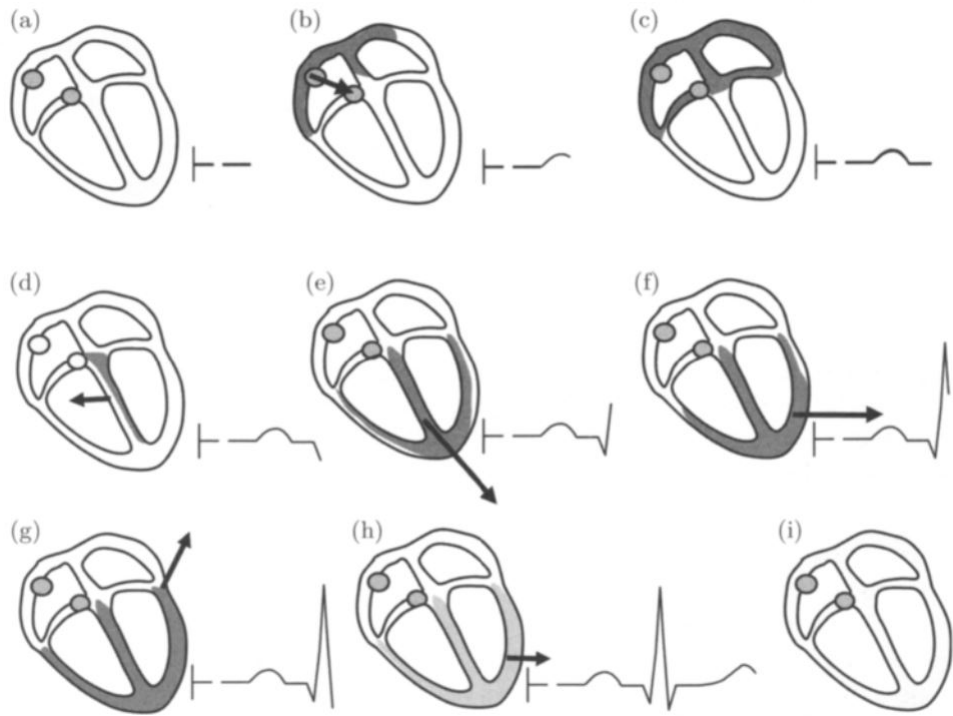


Figure 6: ECG waveform recorded by an electrode placed at the position indicated with the symbol \vdash . (a) All cardiac cells at rest, (b) atrial depolarization, (c) electrical impulse at the A-V node, (d)-(g) ventricular depolarization, (h) ventricular repolarization and (i) all cardiac cells again at rest (from [10])

The PQ segment represents the time during which the electrical impulses travel through the SA node, bundle of His, reaching at the end the Purkinje fibers. This segment is normally isoelectric. The PQ interval corresponds to the period of time during which the atrial depolarization takes place and during which the onset of the ventricular depolarization is produced. The QT interval covers the ventricular depolarization (which occurs simultaneously with the atrial repolarization) and the ventricular repolarization. The TP interval is the time during which the atria and ventricles are relaxed, i.e. are in diastole. Finally, the RR interval corresponds to one cardiac cycle and it is usually used to determine the heart rate [16].

Generally, to measure the alterations in the potentials of the heart non-invasively, electrodes are attached to the skin in different parts of the body. Because there are differences in the way in which the recording of ECG signals is performed for adults and children, and fetuses, following sections review each case.

1.1.4.1 Electrocardiography in Adults and Children In the case of adults and children, the measurement of the electrical activity of the heart is performed through electrodes attached to the skin. The location of the electrodes is chosen so that spatiotemporal alterations can be appropriately measured. In this way, more than two electrodes are generally

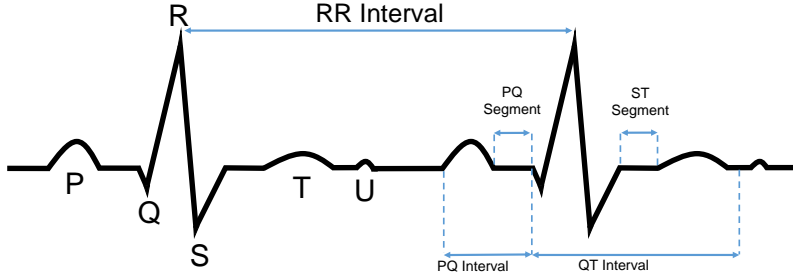


Figure 7: Waves, segments and intervals of the ECG (based on [16])

used to measure the ECG, and the difference of potential between two electrodes is called lead. The standard for the ECG measurement is a 12-lead configuration, for which a total of 9 or 10 electrodes are employed. These leads are classified into three groups: bipolar limb leads, augmented unipolar limb leads and unipolar precordial leads. Unipolar leads are those which capture the activity of a single electrode and they are measured with respect to a reference electrode. Bipolar leads capture the potential difference between two electrodes [10].

To measure the bipolar limb leads (which are denoted *I*, *II* and *III*), electrodes are placed on the subject's arms and on the left leg. Voltages are measured between pairs of electrodes, as mentioned before. Thus, bipolar limb leads are defined according to expressions 1 to 3, where V_{LA} , V_{RA} and V_{LL} refer to the voltage measured on the left arm, right arm and left leg, respectively. These leads describe the electrical activity of the heart in the frontal plane. This is due to the fact that the electrodes used to measure these leads constitute the corners of a triangle (The Einthoven's triangle¹), which has the heart as its center and whose angles are 60° [10].

$$I = V_{LA} - V_{RA} \quad (1)$$

$$II = V_{LL} - V_{RA} \quad (2)$$

$$III = V_{LL} - V_{LA} \quad (3)$$

The augmented unipolar limb leads (*aVF*, *aVL* and *aVR*) are also based on the electrodes used by leads *I*, *II* and *III*. In the augmented leads the voltage measured is the difference between an electrode (a corner of the triangle) and the average of the remaining two voltages (the remaining corners of the triangle). These leads help to fill the 60° gaps of the Einthoven's

¹Willem Einthoven (1860-1927) developed the bipolar limb leads and their corresponding triangle. He also named the waves of the ECG with the letters P, Q, R, S and T. The original design of an electrocardiograph used a galvanometer and the hands and the leg were immersed in saline containers used as electrodes. Einthoven received the Nobel Prize for his discoveries in the field of electrocardiography [16][11]

triangle. The expressions that define the augmented unipolar limb leads are presented in equations 4 to 6 [10].

$$aVR = V_{RA} - \frac{V_{LA} + V_{LL}}{2} \quad (4)$$

$$aVL = V_{LA} - \frac{V_{RA} + V_{LL}}{2} \quad (5)$$

$$aVF = V_{LL} - \frac{V_{LA} + V_{RA}}{2} \quad (6)$$

The unipolar precordial leads provide information about the electrical activity of the heart in the horizontal plane. This lead is recorded with six electrodes in a specific distribution around the torso [11]. Figure 8 shows how the electrodes are placed to obtain the precordial leads, which are named V1, V2, ..., V6. These leads are measured with respect to a central terminal V_{WCT} , which corresponds to the average of the voltages measured on the arms and the left leg, as shown in expression 7. Precordial leads mostly provide information about the activity of the ventricles: V1 and V2 are related with the activity of the right ventricle; V3 and V4 correspond to the anterior wall of the left ventricle, and V5 and V6 reflect the activity of the lateral wall of the left ventricle [10].

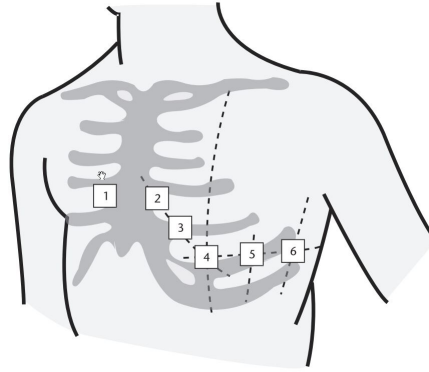


Figure 8: Standard precordial leads (from [11])

$$V_{WCT} = \frac{V_{LA} + V_{RA} + V_{LL}}{3} \quad (7)$$

1.1.4.2 Fetal Electrocardiography

1.1.4.2.1 The fetal heart and its electrical activity It is believed that the human heart beats from the 3rd week of gestation and it also pumps its own blood with its own specific blood type. This is done through an independent circulatory system. By the 20th

gestation week, the heart of the fetus can be heard without any type of amplification and its typical rate is 120-160 bpm [1].

The waves of the fECG are similar to those of the adult ECG. The three components explained for adults (P, QRS complex and T wave) can be identified in the fECG. The morphology of the patterns is also similar. The main difference that exists between the fECG and the ECG in adults is the amplitude of the fECG, which experiences appreciable changes during the pregnancy and even after birth [1].

The electrical activity of the fetal heart appears in the same way as in adults: The same depolarization and repolarization processes take place in the cells of the heart and all the electrical activity starts at the SA node, where the impulses are generated at a specific rate (which is higher for fetuses, as stated before). These impulses travel throughout the heart, reaching the AV node and the other parts of the electrical conduction system of the heart, namely the bundle of His and the Purkinje fibers [17].

In terms of anatomy, the fetal heart has the structure presented before for adults (See Figure 3). The main difference in functional terms is that after birth, as explained before, the left ventricle sends oxygen-rich blood to the body and the right ventricle sends blood to the lungs, so that the blood increases its oxygen content. In the case of the fetuses, however, the oxygen does not come from the lungs but from the placenta. Therefore, there is no need of pumping blood to the lungs for acquiring oxygen, which results in both ventricles of the fetal heart pumping blood throughout the body (including the lungs) [1].

1.1.4.2.2 Measurement of the fetal heart's electrical activity The measurement of the electrical activity of the fetal heart began with the findings of Cremer, who in 1906 could identify the fECG by using vaginal and abdominal electrodes. The original recording is shown in Figure 9, in which it can be barely appreciated the presence of a small change in the signal that corresponds to the fetal electrical activity. Since these experimental results, the fECG has become an interesting signal to many researchers [17]. The measurement equipment used to acquire the first recordings employed the galvanometric devices of that time. These devices had several limitations due to the fact that fetal signals presented a very low amplitude [1].

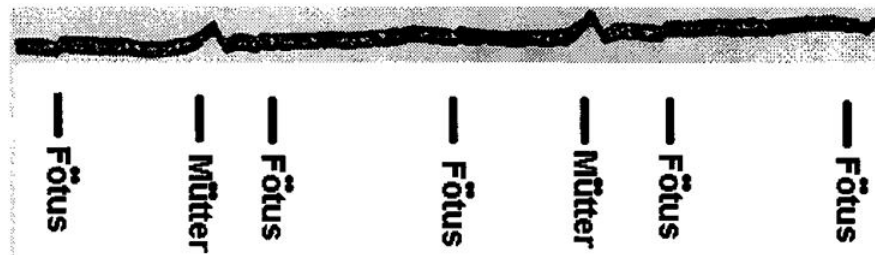


Figure 9: First recorded fECG. The labels “Föetus” indicate the moments where the fECG wave appears and the labels “Mütter” indicate the waveform that corresponds to the maternal component of the measured signal (from [17])

Before 1962, the generalized method for fECG measurement was the use of abdominal electrodes. But because the measured signals showed a very low SNR, these studies did not produce satisfactory results since they did not allow the appropriate identification of the ECG components. In 1963 Hon proposed the use of a vaginal electrode that could be directly attached. This electrode was the precursor of the scalp electrodes that are used nowadays for invasive measurements [17]. According to this, the fECG can be recorded in two ways: invasively through an scalp electrode during delivery or non-invasively through electrodes placed on the abdomen of the mother [18]. To measure with a scalp electrode the skin must be penetrated, which means this method can be used only at the last stage of pregnancy [17]. A disadvantage of the invasive measurement that is worth mentioning is that, since there is just one electrode, this type of measurement allows examining only one dimension of the electrical activity of the fetal heart. Another issue that can affect the measurement with a scalp electrode is the movement of the fetus, which will cause axis movements in the recorded signal. Additionally, the invasive recording of the fECG can be performed only under specific clinical circumstances, which brings a risk to the safety of the fetus [1].

On the other hand, the non-invasive measurement of the fECG can be accomplished at early stages of pregnancy, from the 18th week [1]. In this case the signal that is measured from the abdomen contains the fECG, the mECG component and different types of noise and artifacts such as the maternal electromyogram (mEMG) and her respiratory activity, brain activity of the fetus, the power line interference, baseline wander and random electronic noise [3][2]. There is a time and frequency overlap between the mECG component and the fECG and this makes it impossible to use conventional filtering techniques to extract the fECG from the aECG [4]. Additionally, there are multiple layers of tissue between the fetus and the abdominal electrodes. Some of this tissue has a very low conductivity so that it constitutes a complex path for the fECG as it travels from the fetal heart to the electrodes. Furthermore, some of these tissue layers exist only during certain weeks of the gestation time. One example of this is the vernix caseosa, which is the tissue layer with the lowest conductivity. This layer is formed between the 28th and 32nd weeks of pregnancy. At the end of the pregnancy the vernix caseosa slowly disappears. Other examples of tissue layers that change over the gestation time are the amniotic fluid and the placenta [1].

Another issue that is worth considering is the position of the fetus, which varies during gestation. During the first six months of pregnancy the fetus keeps moving considerably, but during the last three months, there is a settlement and the fetus commonly adopts the vertex position, which is a head-down position. Figure 10 shows some possible presentations of the fetus at the end of gestation. As it can be observed, the vertex position is the most probable but other presentations are also possible. Furthermore, the vertex position, at the end of gestation, has its own alternatives (Figure 11). The main outcome of the different possibilities that exist for the fetal position is that the cardiac signals recorded from the abdomen may vary depending on that position. Thus, because the position is unknown, the recorded abdominal signals cannot be associated to a specific lead [1].

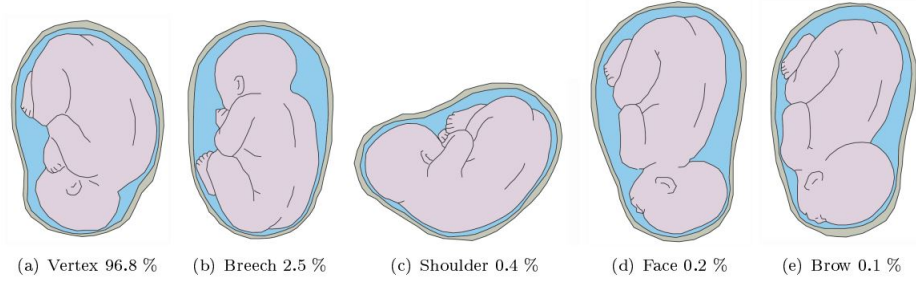


Figure 10: Some fetal presentations with corresponding percentage of incidence (from [1])

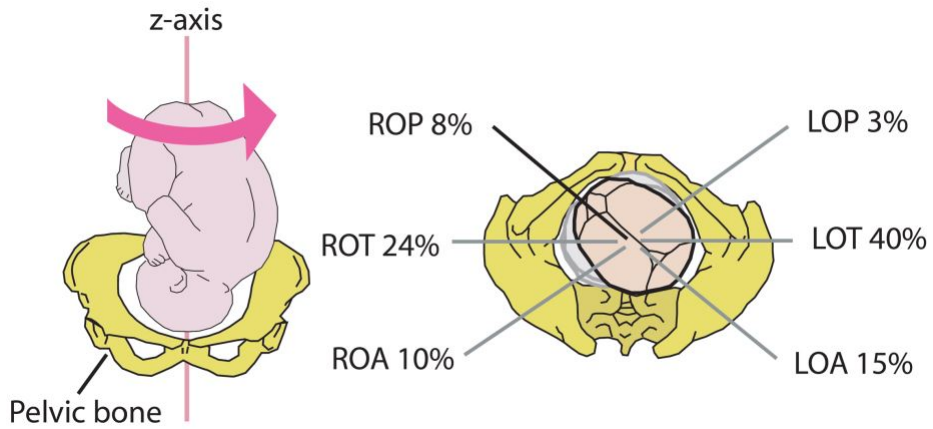


Figure 11: Vertex positions with corresponding percentage of incidence. Abbreviations: L — left, R — right, O — occiput, A — anterior, T — transverse and P — posterior (from [1])

1.1.5 Independent Component Analysis as Blind Source Separation Technique

One of the techniques used in the proposed algorithm is the Independent Component Analysis (ICA). Therefore, it is important to review the most important aspects about the technique and how it can allow the separation of signals.

1.1.5.1 Basic ICA Model The basic ICA model is built under the consideration that several original signals are generated by independent sources. These sources are mixed by a mixing matrix and then are captured by several sensors. These signals captured by the sensors are processed to find a demixing matrix that can lead to the original sources [19]. This is usually illustrated with the *cocktail party* example, in which J different voices are recorded by N microphones. Each of these recordings is a (weighted) linear superposition of the voices. If a digitalized version of the voices contains M samples, then the sources can be represented by a $J \times M$ matrix, S . The signals from the microphones can be also represented with a matrix X with dimensions $N \times M$. Therefore, X is a transformation performed on S (through the propagation of sound waves). This transformation is obtained as the product

between S and the mixing matrix, A [20].

Following previous statement, the ICA model can be represented according to equation 8, where S is the matrix containing all the source signals, A is the mixing matrix with constant elements, and X is the matrix of measured signals.

$$X = AS \quad (8)$$

ICA can be used to recover the source signals by finding a matrix W such that expression 9 can be satisfied, being \hat{S} the estimated source space and the demixing matrix W should be an approximation of A^{-1} [20]. For the estimation of the matrix W , ICA makes two assumptions: (1) source signals contained in S are truly independent, and (2) source signals are non-Gaussian. Another restriction involves the number of measured signals: the mixing matrix must be square, indicating that the number of sources should equal the number of signals in X [19].

$$\hat{S} = WX \quad (9)$$

The reason for the non-Gaussianity condition is that ICA uses higher order statistics to measure independence. The central limit theorem states that the distribution of a sum of independent random variables is more “gaussian” than each of the random variables, implying that independence can be measured by the non-Gaussianity. In practice, ICA minimizes or maximizes a cost function such as mutual information, entropy or kurtosis to find the demixing matrix. This is done in an iterative process, during which for each iteration the independence between the generated estimated sources is measured and the weights of the demixing matrix are adjusted accordingly[20].

There are two restrictions in the ICA technique: The first restriction is that the variances of the sources cannot be determined. This means that ICA provides no information about the energy of the estimated sources and also that the sign of the source cannot be established. The second restriction is that the order of the components cannot be resolved. These restrictions come basically from the fact that in equation 9 there is no information about the sources nor about the mixing matrix [19]. For the present work these restrictions do not have a considerable effect, since the morphology of the extracted signals is what is important for an eventual diagnosis.

1.1.6 Adaptive Filters

Adaptive filters are an important type of filters that are capable of changing their parameters according to certain features of the analyzed signal [21]. These type of filters are used in the developed algorithm in a particular configuration called Adaptive Noise Canceller (ANC) and under an specific optimization algorithm known as Least Mean Square (LMS).

Figure 12 shows the basic structure of an adaptive filter. In these type of filters the goal is to produce an output $y[n]$ that can be as close as possible to the desired response, $d[n]$. This is achieved by reducing the error signal, $e[n]$ to its minimum. The output $y[n]$ is given by the convolution between the FIR filter coefficients, $b_n[k]$, and the input signal, as shown in equation 10, in which L is the length of the filter [21].

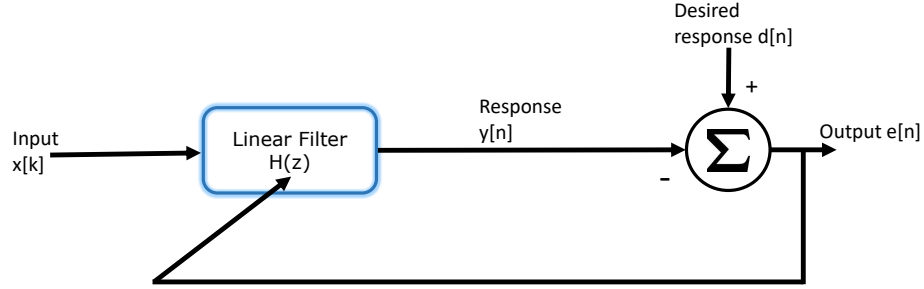


Figure 12: Structure of an adaptive filter (based on [21])

$$y[n] = \sum_{k=0}^{L-1} b_n[k]x[n - k] \quad (10)$$

For the modification of the filter coefficients a gradient optimization method is employed: the Least Mean Square (LMS) recursive algorithm, which uses a recursive gradient method to find the coefficients that minimize the sum of squared error. This method is called steepest-descent. The LMS algorithm produces changes in the filter coefficients based on an estimate of the negative gradient of the error function with respect to $b[k]$ (Equation 11). This equation can be rewritten, after some simplifications, as shown in expression 12. [21].

$$\nabla_n = \frac{\partial e_n^2}{\partial b_n[k]} = 2e[n] \frac{\partial(d[n] - y[n])}{\partial b[k]} \quad (11)$$

$$\nabla_n = -2e[n]x[n - k] \quad (12)$$

The update process of the filter coefficients is as follows: At first arbitrary values are given to them and, then, with each new input sample they are computed again from the new error signal, $e[n]$. The update rule is given by Equation 13, which uses the gradient shown previously in expression 12. In this equation, Δ is a constant that defines the rate of convergence [21].

$$b_n[k] = b_{n-1}[k] + \Delta e[n]x[n - k] \quad (13)$$

1.1.6.1 Adaptive Noise Canceller The Adaptive Noise Canceller (ANC) is a variation of the adaptive filter structure in terms of signal assignation. In this case the input of the structure shown previously in Figure 12 is used to introduce a signal that is correlated with the interference that should be removed. The desired response channel of Figure 12 is used

to introduce the signal that is contaminated with the interference. The output of the ANC is in this case the error signal, which is built as the difference between the signal with noise and the output of the FIR filter. This output should be an estimate of the noise, produced by the action of the filter on the signal that is correlated with the interference. The structure of the ANC is presented in Figure 13.

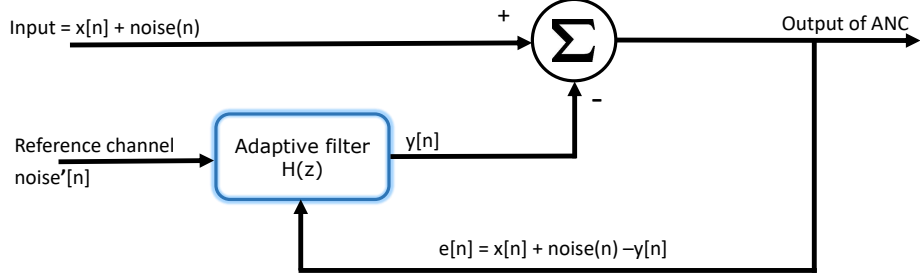


Figure 13: Structure of an Adaptive Noise Canceller (based on [21])

1.2 HISTORICAL FRAMEWORK

This section provides the historical framework for the non-invasive extraction of the fECG. After a brief analysis of the selected documents, a comparison table is presented. The table contains summarized information about the methods, the type of signals used and information on whether or not the method is focused on extracting morphological characteristics from the fECG signal.

1.2.1 Review of Relevant Developments in Non-invasive fECG Extraction

Different approaches have been developed for the non-invasive extraction of the fECG. Most of them are aimed to measure the heart rate of the fetus. Only a few approaches have the extraction of additional morphological characteristics from the fECG as objective. Therefore, it is important to review the different solutions that have been proposed for the problem of the fECG extraction, in order understand the methods that have been applied and their capability to extract more than just the fetal heart rate (fHR).

Partha et al. [22] propose a novel method for the extraction of the fECG from the aECG. The method is based on the principle of the Singular Value Decomposition (SVD). Only one composite maternal ECG signal is required and this method exploits, according to the authors, the feature of the ECG signals of being nearly periodic.

The basic principle of the method is that SVD allows the decomposition of a data matrix into orthogonal component modes. In this way, after configuring data matrices, the method allows the separation through a successive procedure of SVD. For the determination of the dimension of the main matrix A, the Singular Value Ratio (SVR) Spectrum is used. In this case the method can be described through two basic steps: At first, the extraction of the mECG from the aECG by applying SVD to the configured data matrix A, which is arranged so that the consecutive maternal ECG cycles occupy the consecutive rows, and the peak maternal

component lies in the same column. Then comes the extraction of the fECG component, for which a second matrix B is built and in which each row contains one fECG cycle, with the peak value lying in the same column. The SVD technique is applied on B and the extraction of the fECG becomes then possible. For this extraction three approaches are proposed. The difference between these approaches is the way in which the data matrix is configured. For the implementation of the method two datasets are used: One with a high noise level and without slowly varying low frequency component and the other one, obtained from a woman with 37 weeks of gestation, in which there is a low frequency trend component. This trend is eliminated through a preprocessing stage. The method is said to be applicable to the separation of components in any composite signal where the signals can be configured to be algebraically orthogonal to each other.

Richter et al. [23] studied the use of non-linear state-space projections for extracting the fECG from the aECG. Non-linear state projections is a method originally developed for noise reduction in deterministically chaotic signals and its basic principle is the estimation of an “attractor”, and the projection of a trajectory onto it. To create the trajectory, delay coordinates are used. In the case of fECG extraction, the trajectory is built for the ordinary maternal ECG, so that the part that does not correspond to that ECG can be found by determining the deviations from the formed loop (trajectory). In this way, the maternal ECG is separated from the fECG and the random noise. The method is applied again (with different parameters) on the signal that contains the fECG component and the noise to achieve the noise reduction. Results show that under relatively low noise conditions the method performs an appropriate extraction. High noise levels and systematic low-frequency alterations of the baseline can have negative effects on the effectiveness of the extraction.

A combined method is proposed by Ye-Lin et al. [24]. The method uses both thoracic and abdominal signals and it aims to remove the interferences of the fECG a cascade structure. The database used for the development of the method consists on 54 multichannel aECG signals recorded between 21 to 40 weeks of pregnancy. This corresponds to a Physionet database [25]. Figure 14 shows the block scheme of the proposed method. A pre-processing stage for the attenuation of low-frequency components and power-line interference is firstly applied (not shown in the figure). The pre-processed signal is introduced into the cascade scheme and the first step is the removal of the mECG component from the aECG. This is accomplished through an Event Synchronous Canceller (ESC), which uses both thoracic and abdominal signals. Here the thoracic signal is used as reference for the ESC. The Pan-Tompkins algorithm is applied previously on one of the thoracic signals in order to detect the maternal QRS complexes. A scaling process takes place on the mECG signal and a subtraction allows finally the removal of the mECG component. The second step of the method consists on the reduction of the baseline wander. This is achieved through Empirical Mode Decomposition (EMD). After the baseline wander is reduced, the third step starts. In this step ICA is applied to identify the component that contains the fECG. The final step of the algorithm is the fetal QRS complex detection and enhancement. The detection is accomplished by using the Pan-Tompkins algorithm and the enhancement is executed with a technique based on the cross correlation. The performance of the algorithm is measured by means of the fetal QRS complexes detection, which is achieved in 80% of the cases.

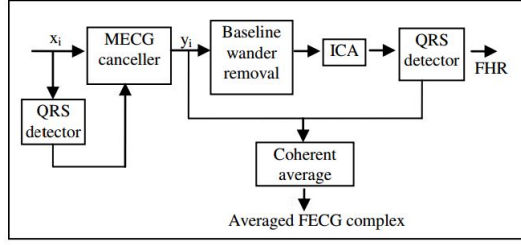


Figure 14: General scheme of the combined method (from [24])

Khamene and Negahdaripour [2] propose a Wavelet-based method for the extraction of the fECG from the aECG. The central point of the method is the detection of the singularities through the modulus maxima of the wavelet coefficients. The modulus maxima is thus used as a way to separate the mECG component from the aECG. The method can be described as a two main steps method, where the first step is the detection of the modulus maxima that represent the singularities. After that, and after correctly discarding the corresponding mECG component, the second main step is the reconstruction of the fECG from its corresponding modulus maxima. The authors introduce two different approaches: one with use of at least one thoracic signal and one with abdominal signals only. In the first approach the thoracic signal is used to determine some a priori information about the location of the modulus maxima of the mECG component. Then, the wavelet transform is calculated and the modulus maxima of the wavelet coefficients are found. A fuzzy-based comparison between the modulus maxima allows the recognition of the modulus maxima that correspond to the mECG, being these discarded. After this, the reconstruction of the fECG from the remaining modulus maxima must be performed. In the second approach the procedure is similar, but, because there is no a priori information about the location of the modulus maxima, all the information is extracted from the abdominal signal. To test the method the authors use both synthetic and real signals. For synthetic signals they report a SNR enhancement between 20 and 40 dB (depending on the simulated gestation time and depending on the approach applied) and for real signals the parameter used to measure the effectiveness is the normalized cross-correlation, which is 0.89 (for approach 1) and 0.79 (for approach 2) in the worst case.

Zarzoso and Nandi [5] present a comparison between one Blind Source Separation (BSS) method and one Adaptive Noise Cancellation (ANC) method. The BSS method is based on higher-order statistics (Independent Component Analysis - ICA) and the ANC procedure implements a Widrow's Multireference Adaptive Noise Canceller (MRANC) approach. In the case of the MRANC, an optimal Wiener-Hopf solution is used as a best case scenario. Both methods are applied on real recordings, which are divided into two groups, having both of them 5 abdominal recordings and 3 thoracic recordings. The BSS method can be divided into two stages: at first Principal Component Analysis is applied for pre-whitening of the data and then, as a second stage, the actual ICA is applied. The MRANC, which uses the Mean Square Error (MSE) as adaptation criterion for the coefficients, uses the thoracic recordings as reference and the aECG signals as primary input. The objective in this case is to find a signal that represents the mECG component present in the abdominal recording, so that it can be subtracted from that recording. In terms of performance, the tested BSS method pro-

vides better quality in the reconstructed signals and it offers components with less noise than those of the MRANC method. Furthermore, the MRANC can be affected by the electrode placement, because it uses the correlation as a parameter for the adaptation. In this way, the BSS technique brings, according to the authors, a superior performance, although it is computationally more expensive than the MRANC technique.

Silva et al. [9] present a summary of the PhysioNet/Computing in Cardiology Challenge 2013. The challenge pretended to stimulate the development and improvement of implemented algorithms for extraction of Fetal Heart Rate (fHR), fetal interbeat intervals (fRR) and fetal QT intervals (fQT). With a total of 53 international teams, the challenge was divided into 5 events. Each event proposed a specific task for the teams (e.g. fHR or fQT computation). The databases used for the contest consisted on a variety of datasets from different databases that were grouped to build a standardized database. The constructed database was divided into three categories: training, open test and hidden test. A special software helped with the scoring process. This software performs a comparison between the reference annotations of the data and the annotations proposed by the teams. Different methods were used in the challenge such as subspace decomposition, wavelet transforms and combinations of different techniques. As a result of the challenge, 91 open-source implemented algorithms are available on the website of Physionet.

Fatemi et al. [26] have developed a method for the extraction of the fECG using a Multistage Interference and Noise Cancellation (MINC). The general scheme of the MINC method is shown in Figure 15. The first stage of the method consists on the typical pre-processing that is aimed to remove common noises and artifacts. After this stages a single channel is selected to be processed by the Denoising by Deflation (DEFL) algorithm, which is responsible for canceling the mECG component from the aECG. The DEFL process applies a transform on the data using π CA to decompose the signal. Then the mECG component is removed and the recomposition of the signal takes place. Hence, at this point the signal is supposed to contain only the fECG component and some remaining background noise. This noise is removed by the next step of the algorithm, which uses Eigenvalue Decomposition (EVD). A final stage enhances the fECG by using a denoiser which is based on the Kalman filter.

To test the method, its ability to detect the fetal QRS complexes is measured and compared to other two methods, namely ICA and ICA with DEFL. The used database is the Physionet Challenge database and to score each method the software WFDB TACH is employed. The reported scores (average errors) are 4150 for ICA, 319 for ICA+DEFL and 170 for the proposed method. This means, according to the authors, that the MINC method outperforms the other compared methods.

Behar et al. [8] propose a Bayesian Filtering Framework based on an Extended Kalman Filter (EKF) for extracting the fECG. The algorithm can be divided into 5 steps: The first step is the prefiltering, which includes a bandpass filter. The second step consists on the application of Single EKF (EKFS). This second step is used to produce a template for the fECG, that is used in the third step. The third step is the use of Dual EKF (EKFD) to separate the three components: mECG, fECG and noise. After this step, the fourth step applies a post-filtering with an additional bandpass. The final step is the SNR computation and the measurement of the QT interval. To test the algorithm artificial signals are generated with the open source

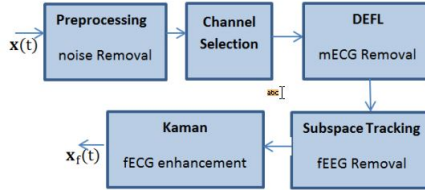


Figure 15: General scheme of the Multistage Interference and Noise Cancellation (from [26])

simulator fecgsyn. 20 one minute signals are generated for training and 200 signals with the same duration are generated for test.

The results of the test show an improvement in the SNR of 1.97 dB after EKFS and 14.14 dB after EKFD. For the QT measurement the median absolute error is calculated, and the reported errors are 17.0 ms for EKFS and 4.0 ms for EKFD.

Behar et. al [18] provide a comparison of different single channel fECG temporal extraction methods. The compared methods are the State Neural Network (ESN) based filtering, the Least Mean Square (LMS), the Recursive Least Square (RLS) adaptive filter and the Template Subtraction (TS) technique. The recordings for the comparison consist on real signals from two databases composing a total of 4 h 22 min of data from nine pregnant women. The importance of the signal preconditioning and in particular the baseline wander cutt-off frequency is also studied and the results suggest that a higher baseline wander high pass cutt-off frequency than traditionally used for fECG analysis significantly increases performance for all evaluated methods. Another finding of the research is that the Signal Quality Indices (SQI) improve the performance of all methods by excluding bad quality chest ECG. The quantitative results demonstrate that the ESN based algorithm performs best on the test data with an F1² measure of 90.2 % as compared to the LMS (87.9 %), RLS (88.2 %) and the TS (89.3 %) techniques.

Panigrahy et al. [3] propose a method for the extraction of the fECG from the single channel aECG. The method is based on the Particle Swarm Optimization (PSO) with Extended Kalman Smoother (EKS) and it is divided into four stages: At first the pre-processing of the data is done. At this stage are removed, with the application of digital filters, the baseline wander and the power line interference. After the pre-processing stage comes the phase assignment stage, in which the maternal R-peaks are detected by using a Shannon energy envelope estimator with Hilbert transform and moving average filter. After the detection of the R-peaks, a specific phase between $-\pi$ and $+\pi$ is assigned to each sample value. As third stage comes the estimation of the optimization parameters for the mECG component in aECG for which the PSO is used. The optimized parameters (amplitude, width and phase) contribute to the modeling process of the mECG envelope. The last stage of the method is the EKS, which is responsible for the estimation of the mECG component in the aECG, so that the mECG can then be subtracted from the signal obtained after the pre-processing stage. Consequently, the output after the subtraction will be the fECG. For the evaluation of

²Parameter obtained from the Positive Predictive Value (PPV) and the Sensitivity (Se)

the method, three parameters are calculated: Sensitivity (93.2 %), positive predictive value (94.97 %) and accuracy (89.7 %). A comparison between the mentioned parameters for the presented method and for some other methods such as Extended Kalman Filter (EKF) with PSO, Extended Kalman Smoother (EKS), EKF and Recursive Least Square (RLS) shows that the presented method provides, in each case, better results than the other evaluated methods.

Ionescu and Hnatiuc [7] present a method for the non-invasive extraction of the fECG and the determination of the corresponding heart rate. The method combines several techniques: ICA, Wavelet transform and Fourier transform to perform the extraction of the fECG from the aECG, without using any thoracic signal. The first stage of the method is the pre-processing, in which filters are applied to remove the power line interference and to reduce high frequency noises mainly from motion artifacts. The second stage applies the ICA technique, particularly the FastICA algorithm. This technique is combined with two pre-processing techniques namely centering and whitening. Through the FastICA algorithm the component that corresponds to the fECG can be found, but it still contains some noise and interferences, such as baseline wander and Electrohysterogram (EHG), which is the electrical activity of the uterus. In the fourth stage digital filtering based on the Kaiser Window is applied. Also, the Undecimated Wavelet Transform (UWT) is employed to remove wideband noise. However, after applying these filters, the SNR can be further improved. The Fast Fourier Transform (FFT) and its inverse are used to achieve a better SNR in the fECG signal. The final stage of the method consists on the fHR estimation.

Nasiri et al. [27] present a method for the extraction of the fECG from the aECG, using two signals: the aECG and a thoracic recording of the maternal ECG. The method is based on Nero-Fuzzy Inference System (ANFIS), which is trained with Particle Swarm Optimization (PSO). The reason for using PSO as training algorithm is basically that it allows a faster convergence than other methods and it avoids resulting stuck at local minimums. The proposed method is focused on finding the transformation that the mECG experiments when traveling from the chest to the abdomen. Hence, with a transformation found for the mECG, finding the fECG consists on subtracting the transformed mECG from the aECG. The structure of the ANFIS is composed by two main parts: the antecedent and the conclusion parts. During training, the objective is to update the parameters of both antecedent and conclusion.

To test the method, the authors use both synthetic and real data and they also perform a comparison to other common methods such as Wavelet-based methods, ICA and ANFIS trained with a conventional method (generally gradient descendental). For the synthetic signals the Percent Root-Mean Square Difference (PRD) is used as a measure of effectiveness in the extraction. The results are 1.1279 for the Wavelet based method, 0.5320 for the simple ANFIS and 0.4734 for the proposed methods. To calculate the parameters that measure the effectiveness, at first the extracted signal is divided into some pulses (which are accommodated as columns of a matrix). For the real data the SNR_{svd} ³ and SNR_{cor} ⁴ are calculated. The comparison is made in this case between Singular Value Decomposition, Wavelet transform, ICA, normal ANFIS and the proposed algorithm. The SNR_{svd} is 0.8854, 0.8291, 1.8226,

³Value calculated using Singular Value Decomposition. It denotes the ratio of the energy in the fECG components to the energy of noise sources

⁴Value calculated after normalization of the matrix rows and defined such that it gives information about how good two columns are correlated

0.8868 and 0.9305 in the mentioned order. The reported SNR_{cor} is 0.1669, 0.1368, 0.3143, 0.1901 and 0.2107 also in the mentioned order. One special benefit of the proposed method is, according to the authors, that only two recorded signals are required and also that extraction can be performed even at early stages of pregnancy.

Nasiri and Faez [28] present the method mentioned before (using ANFIS), but trained with a genetic algorithm. In this case the structure of the method, the tested signals and the results are similar to those of the PSO-trained ANFIS. The PRD is not calculated for the comparison with other algorithms. Instead, the SNR is used as indicator. An SNR_{svd} equal to 0.4900 is the best result of the experimental test as compared to SVD (0.3941), wavelet transform (0.3943), ICA (0.4970) and normal ANFIS (0.4697).

Raoof K. Bsoul [30] implements a simple wavelet-based method for the extraction of the fECG. The author uses the database Direct and Abdominal Fetal Electrocardiogram. The basic structure of the method is depicted in Figure 16. The first step of the method is to filter the signal by applying a bandpass filter. The frequencies for this filter are selected such that the fetal R-peaks are preserved. The second step of the method is the appliance of the Wavelet transform. The selected mother Wavelet is the Haar and it is applied at level two. The reason for choosing this mother Wavelet is, as stated by the author, that it captures the shape of the fetal heartbeat. The third step is the computation of the derivative of the transformed signal in order to find the fast changing peaks. The fourth step is a complement for the previous step, because it complements the task of finding the peaks that correspond to the fetal heartbeats. The last step is the fECG extraction, which basically consists on using the information of the previous step to establish the temporal location of the fetal R-peaks. The effectiveness of the method is measured as its ability to detect fetal heartbeats. The method is tested for five subjects and the accuracy of the heartbeat detection is 87.7 % in the worst case. The average accuracy is 92.1 %. This way of measuring effectiveness of the extraction is based only on the number of detected heartbeats, rather than the correctness of the detection (temporally correctness).

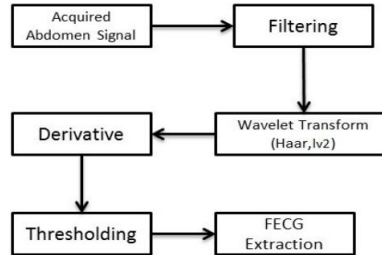


Figure 16: General scheme of the wavelet-based method (from [30])

Jenkins et al. [31] explore the possibilities that adaptive filters may bring in fECG extraction. The authors propose a sequence of adaptive techniques as a solution: Linear Prediction Coding (LPC), Adaptive Noise Cancellation (ANC) and an IIR comb filter. The ANC uses both thoracic and abdominal signals to separate frequency channels of the input and to adapt the

individual frequency components. Then, the LPC, which uses only the abdominal signal, is applied in order to remove uncorrelated noise, by using a time delay. Finally, the IIR comb filter is used to extract the fetal signal. For the experiment the Physionet databases Abdominal and Direct Fetal Electrocardiogram and Non-Invasive Fetal Electrocardiogram are employed. The results of the experiment suggest the the sequence of filters is an effective method to remove the maternal component from the aECG.

An Adaptive Noise Canceller (ANC) based on RLS and Normalized LMS algorithms is explored by Liu et al. [4]. Figure 17 shows the basic block diagram of the adaptive scheme that is used for the mECG cancellation. The primary input, d_k , is the abdominal lead. The thoracic signal is used as reference input (x_k). The output of the system, e_k , is the minimum LS (MLS) estimate, and it should be the fECG component of the primary signal. The weights of the adaptive filter are modified in order to make the output as close as possible to the interference component that the primary input contains. The results of the study show that the RLS-ANC has a better performance than the NLMS-ANC. To measure this performance, the authors calculate the Relative Power Gain (RPG) which helps to determine how fast is the convergence of the noise canceller. For the two mentioned ANCs the RPG curves show that the RLS-ANC converges faster and has a higher tracking ability.

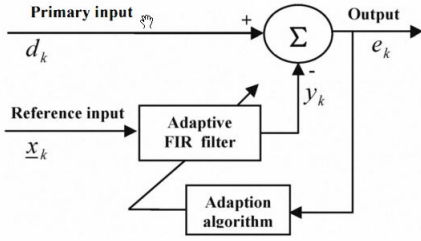


Figure 17: General scheme of the adaptive filtering method (from [4])

Ivanushkina et al. [6] combine the wavelet transform with ICA to develop an integrated approach for fECG extraction. The main reason for using a combined method is that, according to the results of the study, ICA can effectively extract the fECG component, but the noise present in that component makes necessary the use of an additional method, which is in this case the wavelet transform. In that way, the proposed method is composed by two main stages: the extraction of the independent components through ICA, and then the denoising of the independent components through WT. After these two stages, a more complete analysis of the fECG can be performed, for example for the analysis of the different amplitudes and time intervals of the fetal cardiac cycle. To test the method both artificial and real signals are used. The artificial signals are generated from a mathematical model for the fetal cardiac cycle based on gaussian functions, and some changes in the waveform (specially the ST interval) are introduced in order to simulate possible hypoxia in different cases. For the real signals the Abdominal and Direct Fetal Electrocardiogram Database of Physionet is employed. Results show that the extraction is performed appropriately, with low distortion of the fetal cardiac cycle, specially for the artificial signals.

A FastICA-based algorithm is developed by Shehada and Khandoker [32] for the extraction of the fECG from the aECG, without using any thoracic signals. The method can be seen as a two-steps method, in which the first method is the extraction of the mECG component from the aECG, and its corresponding cancellation. This is accomplished by applying the Fast ICA algorithm on the abdominal recordings and then detecting and canceling the maternal R-peaks. The second step of the method is the fECG extraction, for which the output of the previous step is used as input. The Fast ICA algorithm is applied on that input, so that the fECG can be separated from the noise that the signal still contains. A median filter is used to smooth the extracted fECG. To test the method, the Direct and Abdominal Fetal Electrocardiogram Database is used. The ability of the algorithm to detect the fetal R-peaks is measured and the average value of detected R-peaks is 91.4 %. Also, the temporal location of the detected fetal R-peaks is compared to the direct recordings (measured directly on the fetal scalp), and the locations of the R-peaks are close with a correlation coefficient of ρ 0.84 and a p-value equal to 0.

1.2.2 Comparison Table

Table 1 provides a comparison between the methods that were previously analyzed. From the table it is easy to see which methods or techniques are mostly used and which are focused on extracting morphological characteristics from the fECG signal. Also, the table shows if the method uses thoracic signals and the type of data that is employed (real, synthetic or both).

Table 1: Comparison table for reviewed fECG extraction methods

Authors	Title	Used Technique	Extraction of morph. char.	Thoracic signals	Real or synthetic
Partha et al.	Fetal ECG Extraction from Single-channel Maternal ECG using Singular Value Decomposition	Singular Value Decomposition	No	No	Real
Richter et al.	Fetal ECG Extraction with Non-linear State-Space Projections	Non-linear State-Space Projections	No	Yes	Real
Khamene and Negahdaripour	A New Method for the Extraction of Fetal ECG from the Composite Abdominal Signal	Wavelet Transform	No	Yes	Both
Zarzoso and Naudi	Non-invasive Fetal Electrocardiogram Extraction: Blind Separation versus Adaptive Noise Cancellation	Blind Source Separation and Adaptive Noise Cancellation	No	Yes	Real
Silva et al.	Non-invasive Fetal ECG: the Physionet-/Computing in Cardiology Challenge	Several Methods	Yes	Yes	Both
Behar et al.	A Bayesian Filtering Framework for Accurate Extracting of the Non-invasive FECG Morphology	Bayesian Framework based on Extended Kalman Filter	Yes	No	Synthetic
Behar et al.	A Comparison of Single Channel Fetal ECG Extraction Methods	Several Methods	No	Yes	Real
Panigrahy et al.	An Efficient Method for Fetal ECG Extraction from Single Channel Abdominal ECG	Particle Swarm Optimization with Extended Kalman Smoother	No	No	Real
Ionescu and Hnatiuc	Fetal Heart Rate Detection and Monitoring from Non-invasive Abdominal ECG Recordings	Independent Component Analysis and Wavelet Transform	No	No	Real
Nasiri et al.	A New Method for Extraction of Fetal Electrocardiogram Signal Based on Adaptive Nero-Fuzzy Inference System	Adaptive Nero-Fuzzy Inference System trained with Particle Swarm Optimization	Yes	Yes	Both
Fatemi et al.	A Robust Framework for Non-invasive Extraction of Fetal Electrocardiogram Signals	Multistage Interference and Noise Canceller	No	Yes	Both
Raoof	A Simple Non-invasive Approach for Fetal Electrocardiogram Extraction Based on Wavelet Transform	Wavelet Transform	No	No	Real
Jenkins et al.	Adaptive Signal Processing Techniques for Extracting Fetal Electrocardiograms from Non-invasive Measurements	Several adaptive filtering techniques	No	Yes	Real

Table 1

Authors	Title	Used Technique	Extraction of morph. char.	Thoracic signals	Real or synthetic
Ye-Lin et al.	Combined Method for Fetal Electrocardiogram Extraction from Non-invasive Abdominal Recordings	Event Synchronous Canceller, Independent Component Analysis and Empirical Mode Decomposition	No	Yes	Real
Nasiri and Faez	Extracting Fetal Electrocardiogram Signal ANFIS Trained by Genetic Algorithm	Adaptive Nero Fuzzy Inference System trained with Genetic Algorithm	Yes	Yes	Both
Liu et al.	Extraction of Fetal Electrocardiogram using Recursive Least Squares and Normalized Least Mean Squares Algorithms	Recursive Least Squares and Normalized Least Mean Squares as Adaptive Noise Cancellers	No	Yes	Not specified
Ivanushkina et al.	Fetal Electrocardiogram Extraction from Maternal Abdominal Signals	Wavelet Transform and Independent Component Analysis	Yes	No	Both
Shehada and Ahsan	Non-invasive Extraction of Fetal Electrocardiogram Using Fast Independent Component Analysis Technique	Fast Independent Component Analysis	No	No	Real

1.3 USED DATABASES

For the development and test process of the designed algorithm three databases are considered: Abdominal and Direct Fetal Electrocardiogram Database [25], Non-Invasive Fetal Electrocardiogram Database [25] and DaiSy Database [33]. There are some differences between these databases that have to be considered. The following part of the document describes the most relevant aspects of the mentioned databases. All three databases share the same powerline interference frequency (50 Hz) because all signals were recorded in Europe.

1.3.1 Abdominal and Direct Fetal Electrocardiogram Database

This database is commonly used for testing fECG extraction algorithms that have the particularity of using only abdominal recordings to perform the extraction. This database does not contain any thoracic signal. It contains only abdominal recordings measured from the mother's abdomen, and also recordings measured from the fetal scalp. This means that the database provides a means of comparison for the extracted signal and the direct recording. This comparison is performed normally for the temporal location of the fetal R-peaks. Table 2 shows the main features of this database.

Table 2: Main characteristics of the Abdominal and Direct Fetal Electrocardiogram Database

Characteristic	Value
Number of women	5
Gestation time	38 to 41 weeks
Institute	Department of Obstetrics, Medical University of Silesia
Measurement system	KOMPOREL (ITAM Institute, Zabrze, Poland)
Number of abdominal recordings per sample	4
Number of direct recordings per sample	1
Number of thoracic recordings per sample	0
	→

Table 2 ↪

Characteristic	Value
Type of skin electrodes	Ag-AgCl (3M Red Dot 2271)
Type of direct electrode	Spiral electrode
Format of the data	EDF
Sampling rate	1 kHz
Resolution	16 bits
Filtering for power line interference and baseline wander	Yes

The database also contains annotations corresponding to the location of the fetal R-peaks. These were determined by the KOMPOREL system and confirmed by specialists. The location of the electrodes is as follows: four electrodes were placed around the navel and a reference electrode was located above the pubic symphysis. Additionally, there was a common mode reference electrode on the left leg of the pregnant woman.

1.3.2 Non-Invasive Fetal Electrocardiogram Database

This database contains only thoracic and abdominal recordings. It is commonly used by those algorithms that require thoracic signals to extract the fECG. The main aspects of this database are shown in Table 3.

Table 3: Main characteristics of the Non-Invasive Fetal Electrocardiogram Database

Characteristic	Value
Number of women	1
Gestation time	21 to 40 weeks
Institute	ETSE Escuela Técnica Superior de Ingeniería - Universitat de València
Measurement system	Not specified
Number of abdominal recordings per sample	3 or 4
Number of direct recordings per sample	0
Number of thoracic recordings per sample	2
Type of skin electrodes	Ag-AgCl
Type of direct electrode	-
Format of the data	EDF
Sampling rate	1 kHz
Resolution	16 bits
Filtering for power line interference and baseline wander	50 Hz notch filter only

1.3.3 DaISy Database

This database is similar to the Non-Invasive Fetal Electrocardiogram Database. It contains both thoracic and abdominal recordings that can be useful to test fECG extraction algorithms. The main features of this database are presented in Table 4. The major disadvantage of this database is that some parameters such as gestation time and resolution are not specified.

Table 4: Main characteristics of the DaISy Database

Characteristic	Value
Number of women	1
Gestation time	Not specified
Institute	Lieven De Lathauwer
Measurement system	Not specified
Number of abdominal recordings per sample	5
Number of direct recordings per sample	0
Number of thoracic recordings per sample	3
Type of skin electrodes	Not specified
Type of direct electrode	-
Format of the data	dat
Sampling rate	250 Hz
Resolution	Not specified
Filtering for power line interference and baseline wander	Not specified

2 METHODOLOGY

As explained in the introduction of the document, there are several sources of interference that make the extraction of the fECG from the aECG a hard task. Because of that, a methodology for the design of an algorithm for non-invasive fECG extraction should take into account that several authors have contributed to the development of techniques that are aimed to accomplish this hard task. Therefore, the methodology should consider a review of the most relevant advancements, in order to establish which methods are the most effective and which of them have as objective the extraction of morphological characteristics from the fECG. After the review of relevant documents, the methodology should be aimed to the development of the algorithm, which should have a defined structure before it is implemented in a specific programming language. The design-stage contains the filtering of the signals obtained from the databases. Then, the main program should be written for the extraction of the fECG from the abdominal signals. After having a program for the algorithm, its performance should be tested in order to establish how effective it is. Finally, a comparison with other developed algorithms should be performed.

The proposed methodology for the development of the algorithm for non-invasive fECG extraction can be divided into 4 main blocks, which are shown in Figure 18. Each of the stages of the proposed methodology is explained in following subsections.

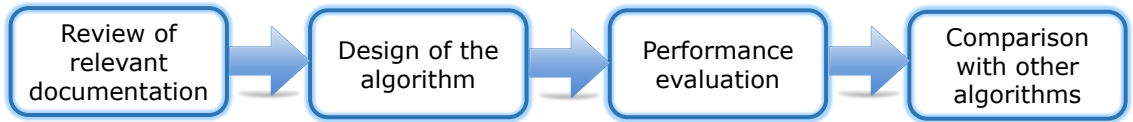


Figure 18: Block diagram of the proposed methodology

2.1 Review of Relevant Documentation

This stage of the methodology includes a complete review of the most relevant approaches that have been proposed to address the problem of the non-invasive fECG extraction. An important factor of this review is the fact that not every approach has as objective the extraction of morphological characteristics, but the extraction of the fetal heart rate (fHR). This makes necessary a classification of the selected documentation, so that it can be easily determined which approaches are aimed to extract morphological characteristics different from heart rate. The selection of the documents is made according to their relevance (sort by relevance), and also according to the number of times that the document has been cited.

The review of the different approaches and techniques proposed by other authors was presented in the reference framework of this work. Each of the considered approaches was analyzed,

and classified according to whether or not the extraction of morphological characteristics is the main goal. At the end of the review a comparison table is presented. This table identifies the important parameters and conditions that describe the each method.

2.2 Design of the Algorithm

The design of the algorithm of the non-invasive fECG extraction is the main stage of this work. The review of the previous solutions to the problem of fECG extraction was useful to have an idea about which techniques could be effective for extracting the fECG from the aECG.

2.2.1 Pre-Processing Stage

This stage considers all the processing techniques that had to be applied on the signals of the databases. Basically the objective is to remove unwanted components such as the baseline wander and the powerline interference.

2.2.1.1 Baseline Wander Removal Baseline wander is a common issue in ECG signals. When a baseline wander is contained in an ECG signal, there are changes in the morphology of the cardiac signals that do not have cardiac origin, for example due to movement of the patient. The frequency content of the baseline wander is commonly below 0.5 Hz. However, some factors can contribute to the presence of baseline wander in higher ranges. This gives some complexity to the problem of removing this interference [10]. Two common techniques for baseline removal were considered for this work: LTI-FIR filters and polynomial fitting. They were implemented in MATLAB and the results were compared in order to find out which method could contribute the most to the removal of the baseline wander. It must be taken into account that generally the literature specifies the use of the mentioned methods for the normal ECG and in this case the filters are applied on abdominal signals, which have different characteristics in terms of amplitude and frequency contents as compared to the normal, standard ECG.

In order for the filters to be tested under the same conditions, the same signal is used. This signal corresponds to the first 10000 samples of one of the abdominal signals of the Non-Invasive Fetal Electrocardiogram Database. The signal is shown in Figure 19 and the corresponding spectrum is shown in Figure 20. The frequency contents of the signal shows that there are components in frequencies below 0.5 Hz, having some of them a considerable amplitude. The spectrum of the signal was obtained using the Fast Fourier Transform.

2.2.1.1.1 LTI-Filtering In order for the signal to remain undistorted, a linear phase response is desired for the LTI filter. That is the reason why it is a better option to consider an FIR filter instead of an IIR filter. The guaranteed stability of FIR filters is also an important factor [10]. Although these type of filters need more coefficients than the IIR filters, distortion should not be allowed because the waveform is an important aspect of this work. Thus, an FIR high pass filter should be designed for the reduction of the baseline wander.

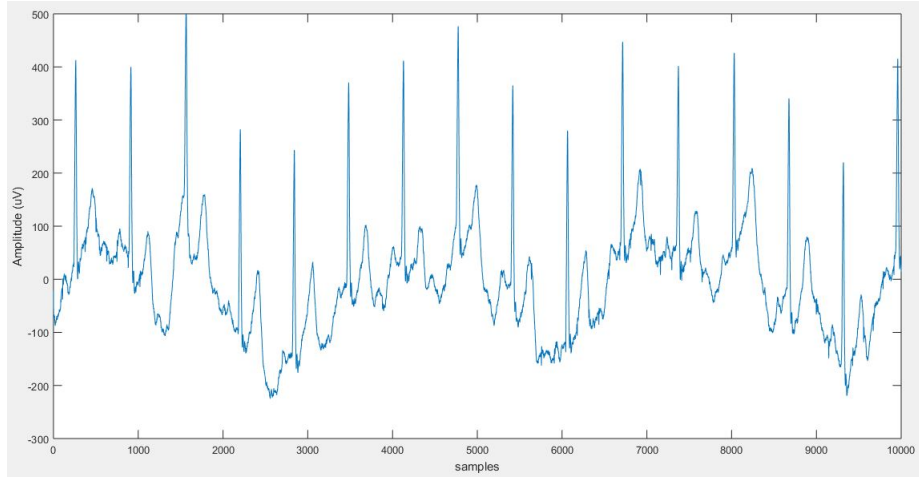


Figure 19: Example of abdominal signal from Non-Invasive Fetal Electrocardiogram Database

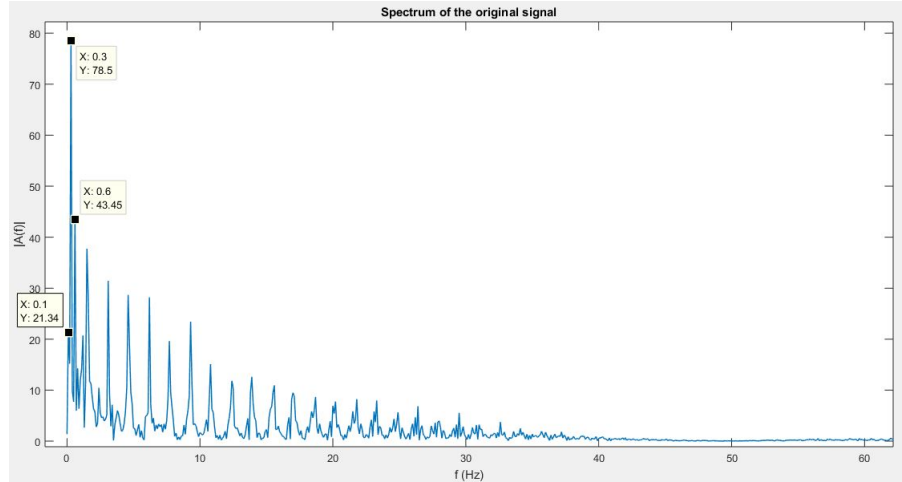


Figure 20: Spectrum of the original signal from Non-Invasive Fetal Electrocardiogram Database

The design of the high-pass FIR filter should be based on the lowest frequency present in the ECG, which is assumed to be related to the lowest possible heart rate. This lowest value appears under the condition of bradycardia, for which a heart rate of approximately 40 beats/minute can be reached. This heart rate corresponds to a frequency of 0.67 Hz, but because of the variability of the heart rate, it is suggested to use a slightly lower cut-off frequency (0.5 Hz) [10].

For the design of the high-pass FIR filter the MATLAB's function *fir1* was used. The order of the filter was chosen according to the recommendations found in [10], which specify that for a minimum stopband attenuation of 40 dB an order of 1884 should be chosen. The order was set to 2000 expecting the stopband attenuation to be greater than 40 dB. The cut-off frequency for the filter was set to 0.5 Hz, and a Hamming window was employed (default option).

Although the attenuation in the stopband was supposed to be at least 40 dB, the frequency response of the filter shows that the attenuation barely reaches 16 dB. For this reason the order of the filter was increased to 2500 to reach at least 20 dB in the stopband. For this case the result is shown in Figure 21.

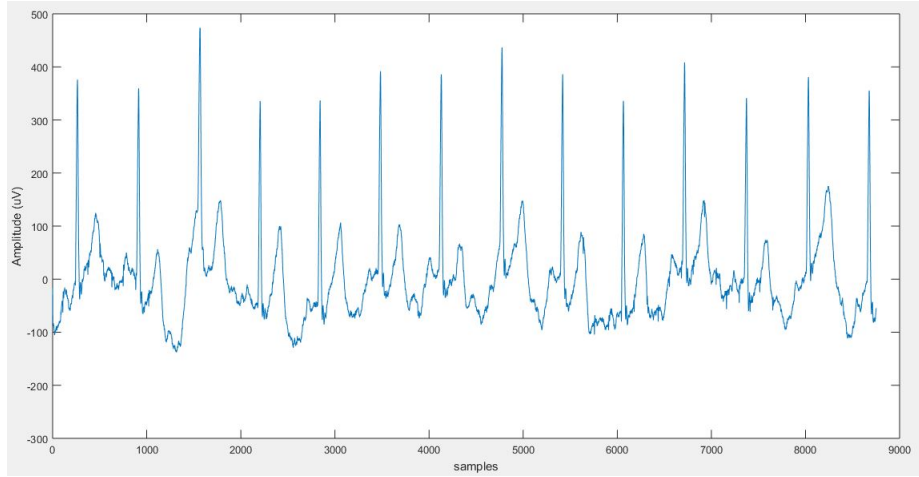


Figure 21: Result of FIR filter on abdominal signal

2.2.1.1.2 Polynomial Fitting In this approach a polynomial is fitted to some representative samples of the ECG signal. These samples (knots) should meet the requirement of belonging to the isoelectric line, which is commonly represented by the PQ interval. The polynomial should reach each of the knots, but it should not be just one line connecting all the knots, because this would result in a poor capacity to track variations. That is a reason why higher order polynomials should be considered. A particular option of this is the cubic spline baseline estimation, in which a third-order polynomial is determined for consecutive triplets of knots [10].

For this method to be appropriately applied, the PQ intervals must be firstly determined. However, after several tries it was concluded that the detection of the PQ interval becomes a very hard task for abdominal signals because of the difficulty that exists for the extraction of the P waves, which are in some of the signals very weak. Therefore, the Q-peaks and some of the S-peaks are used as knots for the polynomial fitting. Some S-peaks were considered at the beginning of the signal for having a better approximation of the baseline wander in the first part of the signal. The result of doing it so is an acceptable approximation for the baseline as can be observed in Figure 22. The signal obtained after subtracting the estimated baseline from the original signal is shown in Figure 23. An additional consideration had to be taken for the polynomial fitting: After subtracting the estimated baseline from the original signal, an offset is added. Thus, the mean value of the obtained signal had to be subtracted from the signal.

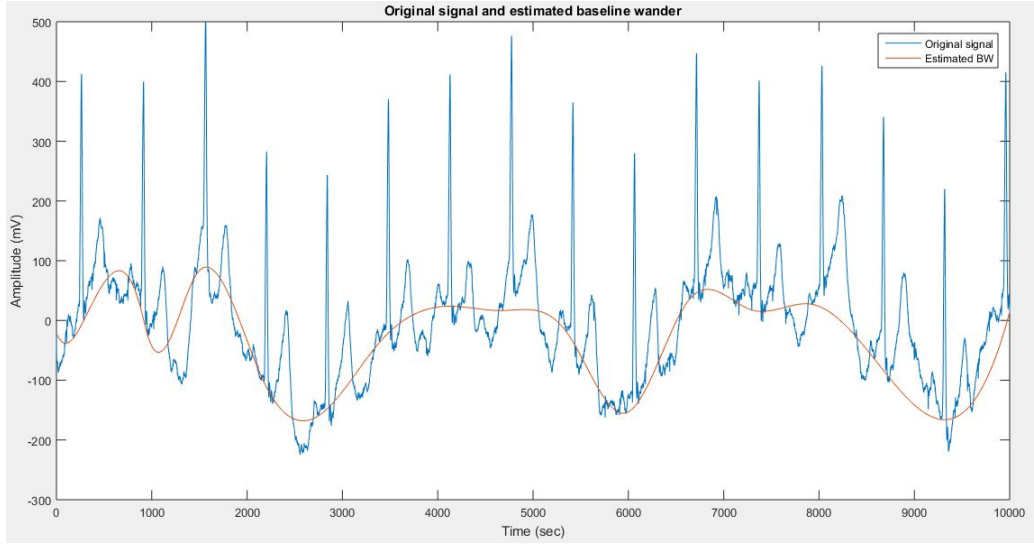


Figure 22: Estimated baseline through polynomial fitting

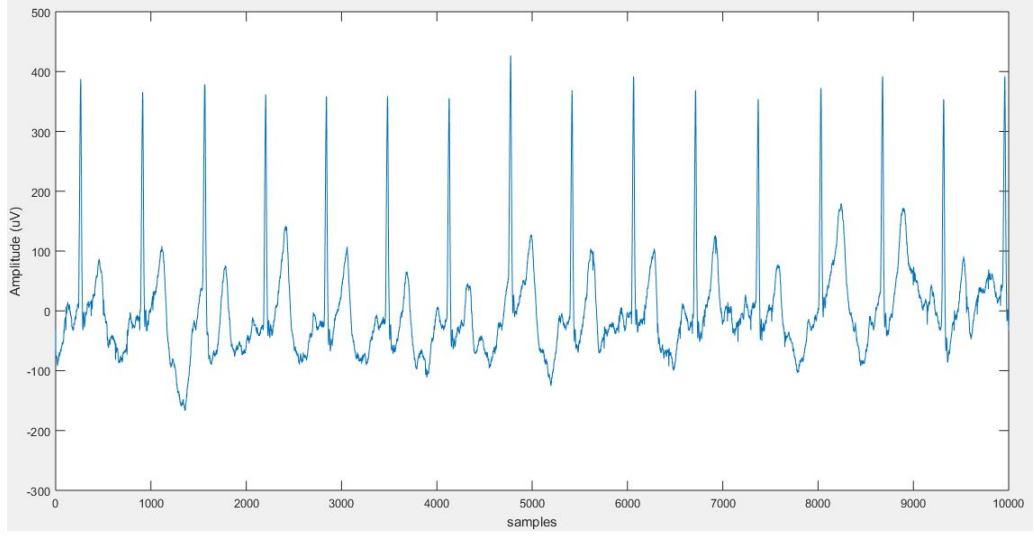


Figure 23: Result of polynomial fitting

Because this type of filter depends on the knots, the QRS complexes of the input signal should be identified first. To achieve this, the Pan-Tompkins algorithm is employed. In this algorithm, a band pass filter is firstly applied between 5 and 11 Hz in order to limit the ECG to the range of the maximum signal energy. This filter also helps to reduce the effect of different types of noise and interferences. After the bandpass filter a differentiator is used to obtain information about the slope of the QRS complex and also the squaring operation is applied. The squaring procedure contribute to two aspects: it increases the slope of the frequency response curve of the derivative and also helps to avoid false detections caused by certain types of T waves. Then a moving average is employed to produce a signal that con-

tains information about both the slope and the width of the QRS complex and, finally, the output of this moving average is passed through a thresholding stage for the detection of the peaks. The total delay of the described processing techniques is considered in order to align the found peaks with the original signal [34][35]. Figure 24 shows the block diagram with the mentioned stages. With this algorithm the three peaks of the QRS complex can be determined.

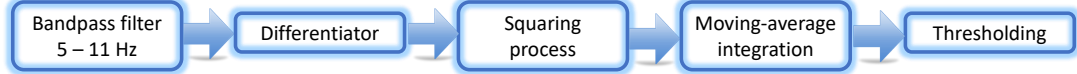


Figure 24: Block diagram of the Pan-Tompkins algorithm (Built from [35])

Experimental results showed that the polynomial fitting is able to estimate the baseline in an appropriate way. However, this is true only when the QRS complexes can be correctly determined through the Pan-Tompkins algorithm. In very noisy abdominal signals and in abdominal signals with certain uncommon morphological characteristics there are some QRS complexes for which the detection is not accomplished. This causes the polynomial fitting to have intervals for which the estimated polynomial does not follow the baseline. Furthermore, the polynomial can describe in some cases abrupt changes that produce a very distorted output signal (Figure 25).

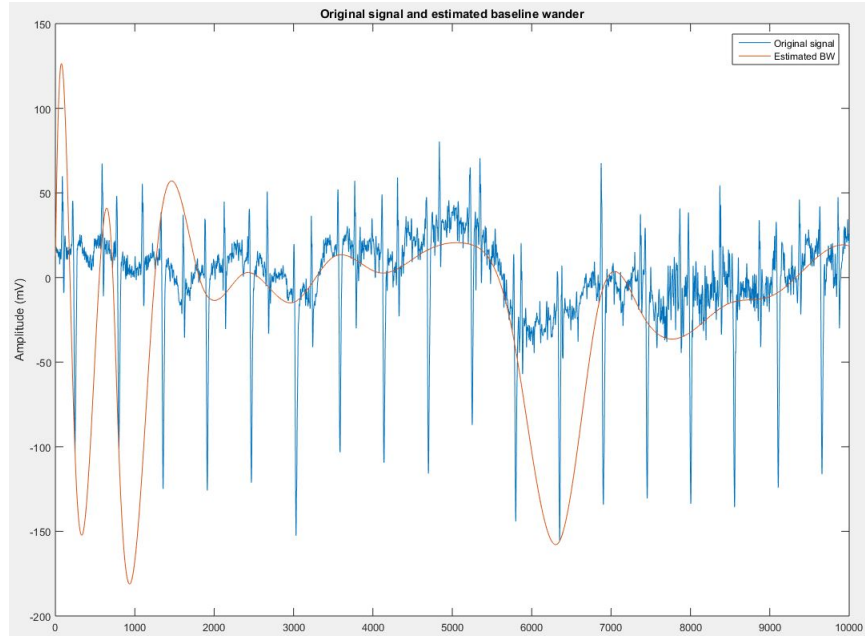


Figure 25: Example of erroneous estimation of baseline when some QRS complexes are not detected

Because of the situation described before, two possibilities for removing the baseline wander

are implemented: (1) If all of the QRS complexes are correctly determined, then the polynomial fitting is applied and (2) if some of the QRS complexes cannot be detected, then the high-pass FIR filter is applied. This implies that the first step of the filtering process must be the QRS complexes analysis through the Pan-Tompkins algorithm. If the intervals between consecutive found peaks deviate too much, then the conventional FIR high-pass filter must be applied.

2.2.1.2 Powerline Interference Removal In order to remove the 50 Hz interference contained in some of the signals, a notch FIR filter was designed and applied on them. The number of taps of the filter was set to 800 so that an attenuation of at least 40 dB could be reached at the center frequency. Figure 26 shows the magnitude response of the designed filter and Figure 27 shows its phase response.

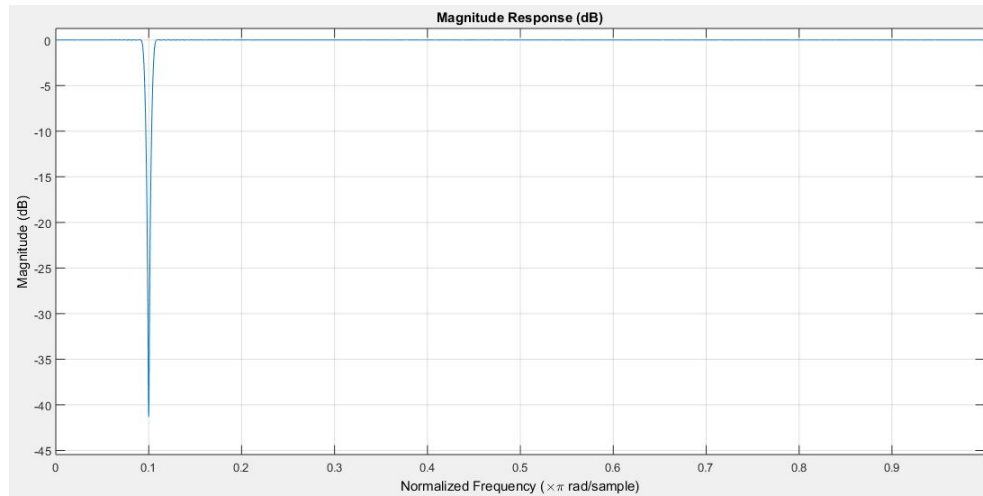


Figure 26: Magnitude response of notch FIR filter used for powerline interference removal

2.2.2 Extraction Algorithm

For the extraction of the fECG signal two approaches are proposed. The first approach employs both thoracic and abdominal signals to perform the extraction. The second approach uses abdominal signals only. Both approaches are based on Independent Component Analysis and Adaptive Filters.

2.2.2.1 First Approach - fECG Extraction Using Thoracic Signals This approach can be explained as follows: Through the ANC and the ICA blocks two different estimates of the fECG are produced. Most of the information the ICA estimate provides is about the R-peaks, while the ANC estimate is expected to provide more information about the fECG waveform different from the R-peaks. The fECG generator combines both of the estimates and produces an fECG signal that can lead to the estimation of parameters apart from just the fHR.

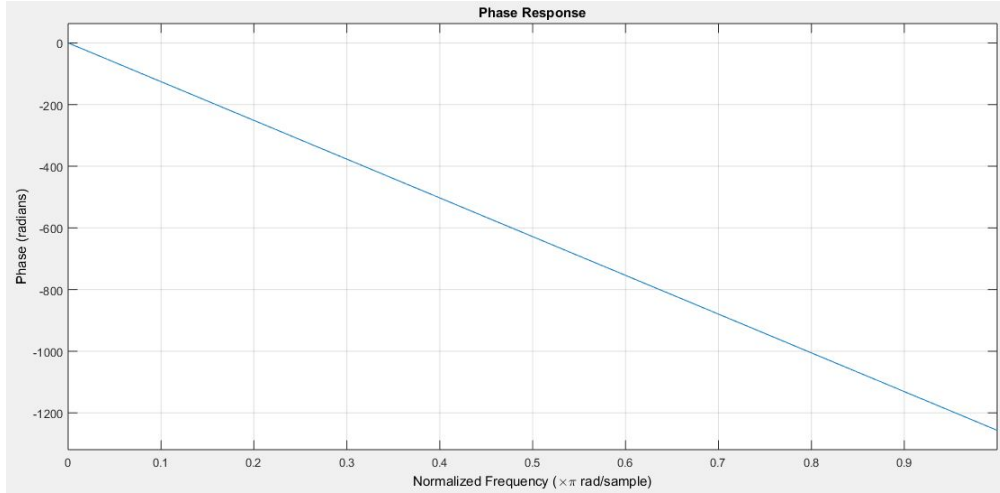


Figure 27: Phase response of notch FIR filter used for powerline interference removal

The basic scheme of the first approach is depicted in Figure 28. There are three major blocks that constitute the approach, namely the ANC, the ICA Analysis block and the fECG Generator. The basic operation of the algorithm can be described as follows: The abdominal signals are introduced in both the ANC and the ICA analysis blocks. The ICA generates an estimation of the fetal independent component (a single signal) based on those abdominal signals only. The ANC block, on the other hand, needs one thoracic signal to be introduced as reference signal in order to generate an estimation of the fECG for each abdominal signal, which means that at the output of the ANC block there will be one signal for each abdominal signal. One of these signals is chosen according to their quality and at the fECG Generator the ICA output and the selected ANC output signal are mixed to generate a new signal that combines the characteristics of both signals. Finally, a smoothing process is performed in to enhance the resulting signal. Each block shown in Figure 28 is explained in more detail now.

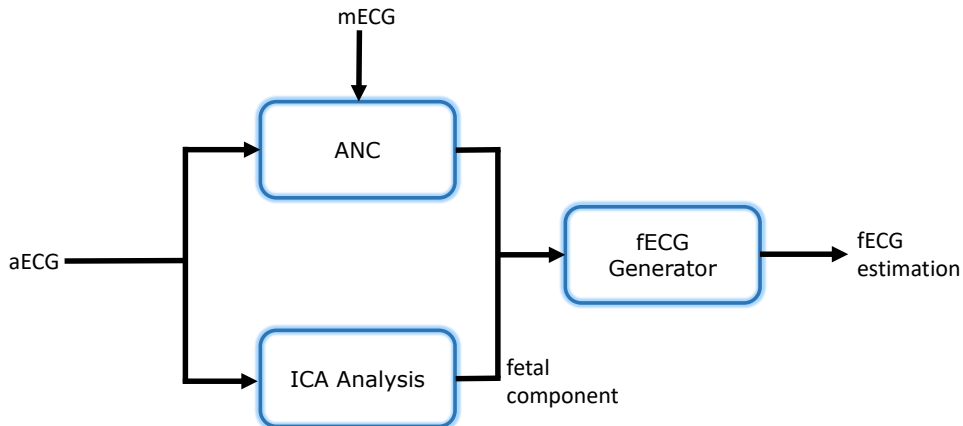


Figure 28: First Proposed Approach - fECG Extraction Using Thoracic Signals

2.2.2.1.1 ANC Block The ANC is an Adaptive Noise Canceller based on the Least Mean Square (LMS) algorithm. The ANC uses the thoracic signals to cancel out the component in the aECG signals that is correlated with those thoracic signals, i.e. the maternal component. In this way, the output of the ANC should ideally contain only the fECG component along with the noise that could not be removed during the pre-processing stage. Figure 29 shows again the basic structure of the employed ANC. In this case the abdominal signals are introduced in the signal channel ($x(n)$ is the fECG with noise and $N(n)$ is the maternal component), and the thoracic signal is sent through the reference channel (signal $N'(n)$). The adaptation of the filter coefficients leads to a signal $N^*(n)$ which should be an appropriate approximation of $N(n)$. Thus, the output of the ANC (in this case the error signal $e(n)$) should be the fetal signal (combined with some noise).

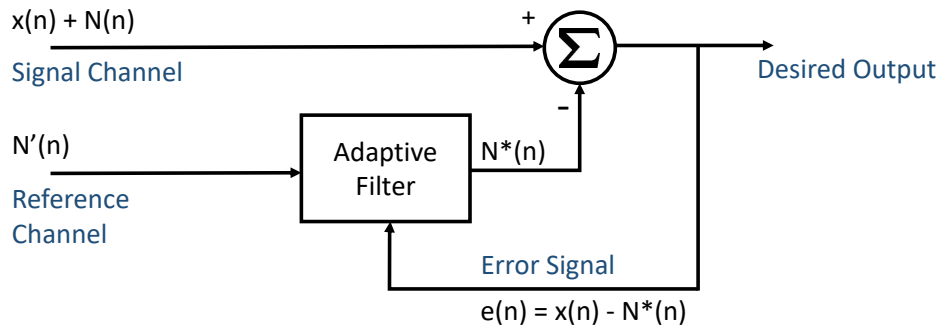


Figure 29: Basic structure of the implemented ANC. Each abdominal signal is introduced to the ANC to remove the maternal component

Because at the output of the ANC there are several signals (as many as abdominal signals), one of the output signals must be selected for the further processing performed by the fECG Generator block. This is achieved based on the detection of the peaks through the Pan-Tompkins algorithm. Basically, the most prominent R-peaks are searched. For each of the signals that come from the output of the ANC the peaks are detected and their quantity and standard deviation for both time and amplitude are measured. Through a threshold a decision can be taken about which of the signals offers the best information for the further analysis. If none of the set of peaks found meets the requirements, then the signal with the greatest maximum value will be chosen as the best ANC output. Algorithm 1 shows the procedure for detecting the best output of the ANC, assuming that the thresholds have been introduced previously.

2.2.2.1.2 ICA Analysis In this block two Independent Component Analysis (ICA) algorithms are employed to extract the independent components (IC) from the abdominal signals. Each of the algorithms builds several independent components, one of which should correspond to the fetus. The fetal IC is automatically detected for each ICA algorithm and after that the best fetal IC is selected based on the waveform. The detection of the fetal IC is based on procedure that uses the output of the ANC. The identification of the best fetal IC is based on how similar the components are to a typical ECG heartbeat i.e. how apt the signal

Algorithm 1 Basic algorithm for detection of best ANC output

```

1: procedure DETECTBESTANCOUTPUT(ANCoutputs)
2:   for i = 1 to Amount Of ANC outputs do
3:     CurrSignal  $\leftarrow$  ANCoutputs(i)
4:     SomePeaksLocation  $\leftarrow$  PanTompkins(CurrSignal)
5:     NumPeaks  $\leftarrow$  length of SomePeaksLocation
6:     LocationStd  $\leftarrow$  Standard deviation of SomePeaksLocation
7:     AmplitudeStd  $\leftarrow$  Standard deviation of CurrSignal(SomePeaksLocation)
8:     MaxAmplitude  $\leftarrow$  maximum value of CurrSignal
9:     if NumPeaks > Threshold1 then
10:       if LocationStd < Threshold2 then
11:         if AmplitudeStd < Threshold3 then
12:           return i
13:     else
14:       Maxima(i)  $\leftarrow$  MaxAmplitude
15:   return i for which max(Maxima)

```

is for providing morphological information about the fetal signal. This identification is made by using a matched filter with a typical ECG heartbeat as template. Figure 30 shows the structure of the ICA analysis block.

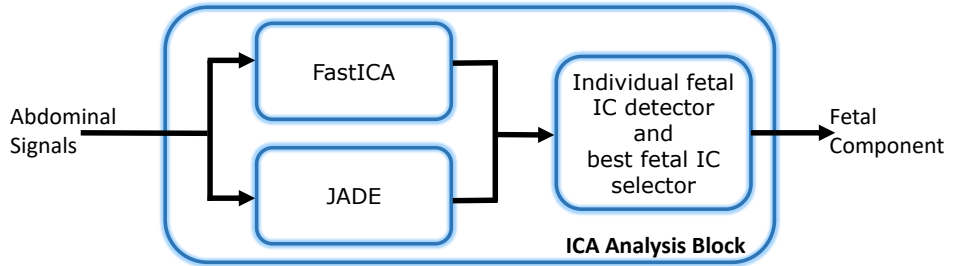


Figure 30: Basic structure of ICA Analysis block

The two ICA algorithms used are the FastICA algorithm [36] and the JADE⁵ algorithm [37][38], for which an implementation made by the authors is available online. The structure of the block allows more algorithms to be added.

As stated before, the fetal component should be automatically detected so that it can be used in the fECG Generator block. This detection is based on two identification mechanisms: The first mechanism is based on the use of the Pan-Tompkins algorithm on each of the components to detect possible R-peaks. The detected peaks are compared to the peaks detected in one thoracic signal and those detected in the best signal of the ANC. If the peaks detected

⁵Joint Approximation Diagonalization of Eigen-matrices

in one component have similar locations to those from the peaks detected in the output of the ANC, if the amount of peaks is greater than the amount of peaks found in the thoracic signal, if the standard deviation of the location of the peaks is under a threshold and if the peaks are close enough to represent the fetal RR intervals, then that component is assigned as the fetal component. Because the separated independent components do not necessarily have the correct sign or polarity, this aspect is evaluated in the function. Both the location of the peaks detected from the component and from its inverted version are compared to the peaks from the ANC signal to decide whether the component should be inverted or not. For this first mechanism of identification the pseudocode is shown in algorithm 2, where it is assumed that the constant values for thresholds and tolerance have been already introduced.

Algorithm 2 Basic algorithm for detection fetal component

```

1: procedure DETECTFETALIC(IndComps, ThoracicSignal, BestANCOOutput)
2:   MaternalPeaksLocation  $\leftarrow$  PanTompkins(ThoracicSignal)
3:   MinMaternalInterval  $\leftarrow$  Minimum distance between MaternalPeaksLocation
4:   NumMaternalPeaks  $\leftarrow$  length of MaternalPeaksLocation
5:   BestANCOOutputPeaksLocation  $\leftarrow$  PanTompkins(BestANCOOutput)
6:   Ranges  $\leftarrow$  BestANCOOutputPeaksLocation  $\pm$  Tolerance
7:   for i = 1 to Amount Of ICs do
8:     CurrSignal  $\leftarrow$  IndComps(i)
9:     SomePeaksLocation  $\leftarrow$  PanTompkins(CurrSignal)
10:    MinInterval  $\leftarrow$  Minimum distance between SomePeaksLocation
11:    SomePeaksLocationInverted  $\leftarrow$  PanTompkins(-CurrSignal)
12:    NumberOfMatches  $\leftarrow$  find matches between (SomePeaksLocation, Ranges)
13:    NumberOfMatchesInv  $\leftarrow$  find matches between (SomePeaksLocationInverted, Ranges)
14:    if NumberOfMatches > NumberOfMatchesInv then
15:      Sign = 1
16:    else
17:      Sign = -1;
18:    NumPeaks  $\leftarrow$  length of SomePeaksLocation
19:    LocationStd  $\leftarrow$  Standard deviation of SomePeaksLocation
20:    AmplitudeStd  $\leftarrow$  Standard deviation of CurrSignal(SomePeaksLocation)
21:    if NumPeaks  $\geq$  NumMaternalPeaks - Tolerance AND NumPeaks  $\leq$ 
        NumMaternalPeaks + Tolerance then
22:      if LocationStd < threshold1 AND AmplitudeStd < threshold2 then
23:        if  $1.25 \times \text{MinInterval} < \text{MinMaternalInterval}$  then
24:          return i, Sign
25:        else
26:          return No signal found

```

The second mechanism for the detection of the fetal component is the same as the previous one, except that it does not consider the ANC signal. This means that if there is no ANC signal available the detection of the fetal component is based on the amount of peaks, their standard deviation (in both time and amplitude) and the minimum interval that exists

among the detected peaks. Given the similarity with the first mechanism of detection, the pseudocode for this case is omitted.

The fact that the ICA Analysis block is seen as a best output system implies that some criteria is implemented to decide which of the fetal components is the best option. This criteria is basically the similarity with a typical heartbeat waveform. This brings the advantage of choosing the component that is closest to a cycle that contains the well known P, Q, R, S and T waves. This does not mean that the fetal component must contain a perfect representation of the typical heartbeat, but it means that from the available components the one with the most similar waveform to that typical heartbeat will be chosen.

To measure the similarity a matched filter is applied. This matched filter is implemented as an FIR filter, as shown in Figure 31. The template for the matched filter is a typical ECG template, which is generated with the ECG simulator *ecgsyn* [39]. The template is time-reversed and the result is used as the impulse response of the FIR filter. Algorithm 3 shows the basic pseudocode for the detection of the best fetal IC.

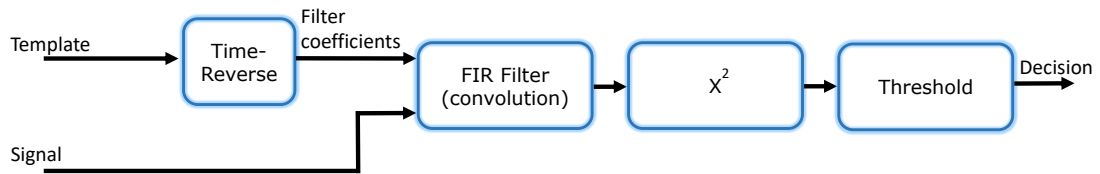


Figure 31: Structure of the matched filter used for selection of best fetal component

Algorithm 3 Basic algorithm for detection of best fetal component

```

1: procedure DETECTBESTFETALIC(FetalICs, Template)
2:   b  $\leftarrow$  Invert in time Template
3:   for i = 1 to Amount Of Fetal ICs do
4:     CurrSignal  $\leftarrow$  FetalICs(i)
5:     FilteredSignal  $\leftarrow$  Convolution (b, CurrSignal)
6:     SquaredOutput(i)  $\leftarrow$  FilteredSignal2
7:   NormalizedOutput  $\leftarrow$  Normalize using max. value(SquaredOutput)
8:   for ii = 1 to Amount Of Fetal ICs do
9:     Peaks  $\leftarrow$  find peaks above threshold for NormalizedOutput(ii)
10:    NumPeaks(ii)  $\leftarrow$  length of Peaks
11:   return Index for which max(NumPeaks)
  
```

2.2.2.1.3 fECG Generator This block is responsible for mixing up the best signal produced by the ANC and the best fetal component selected with the algorithm described previously. This mixing process is performed through the mean of both signals. This is made

because the mean allows to amplify the segments that are common to both signals. For example, if both signals, in a certain interval, contain a presumable fetal T wave that can barely be identified because of the low amplitude, the mean of the signals in that interval will provide a segment with a higher amplitude than if only one of the signals contained a presumable T wave. In this way, the mean produces a signal that mixes the information from both input signals, with a higher amplitude in the intervals during which both signals share a similar waveform.

After the mean is computed, a smoothing process is performed in order to produce a signal with an improved waveform that can be better analyzed by a specialist. The Savitzky-Golay filter is used for smoothing the resulting fetal signal. The order of the filter is set to 5 and the frame length is set to 21. These parameters were adjusted heuristically so that the ECG waveform is not majorly modified.

2.2.2.1.4 Implementation of the algorithm The implementation of the algorithm was made in MATLAB for the two databases that contain thoracic signals (Non-Invasive Fetal Electrocardiogram Database and DaISy). Figure 32 shows the map of functions and scripts that were used for the implementation of the first approach for the DaISy database. For the other databases the structure is essentially the same. The only change is the main script (in the middle of the diagram). The functions *fastica* and *jadeR* are MATLAB implementations created by the authors of the algorithms [36][37][38].

2.2.2.2 Second Approach - fECG Extraction Without Using Thoracic Signals
The second approach does not use any thoracic signal. From the abdominal signals it determines the fECG by employing slightly modified versions of both of the blocks described for the first approach, namely the ANC and the ICA Analysis. The scheme of the algorithm is shown in Figure 33.

The ICA technique requires certain noise conditions in order to work. In some cases there is not a component with only fetal cardiac activity. Instead, in these cases there is a component that contains activity from both fetus and mother. However, ICA allows the extraction of a maternal component that contains only low fetal activity. For this reason, the second approach exploits the ICA technique as a method to extract the maternal component instead of the fetal component for the further analysis. This approach works as follows: The ICA block receives the abdominal signals and produces a set of ICs, one of which is an approximation for the maternal component. This component is used as reference in the ANC block. The ANC outputs are enhanced so that most of the maternal component is removed from each of the abdominal signals. To achieve this enhancement, the R-Peaks of the maternal component are found and used in a procedure that aims to approximate the QRS complexes of the output of the ANC (not the actual output signal, but the output of the FIR filter, y) to those of the abdominal signals. With this enhancement a signal that represents the fetal activity in a better way is achieved. The reason for implementing the described enhancement of the ANC is that it is not always capable of producing a signal that is similar enough to the maternal component of the abdominal signal, producing thus a signal that contains the activity of both

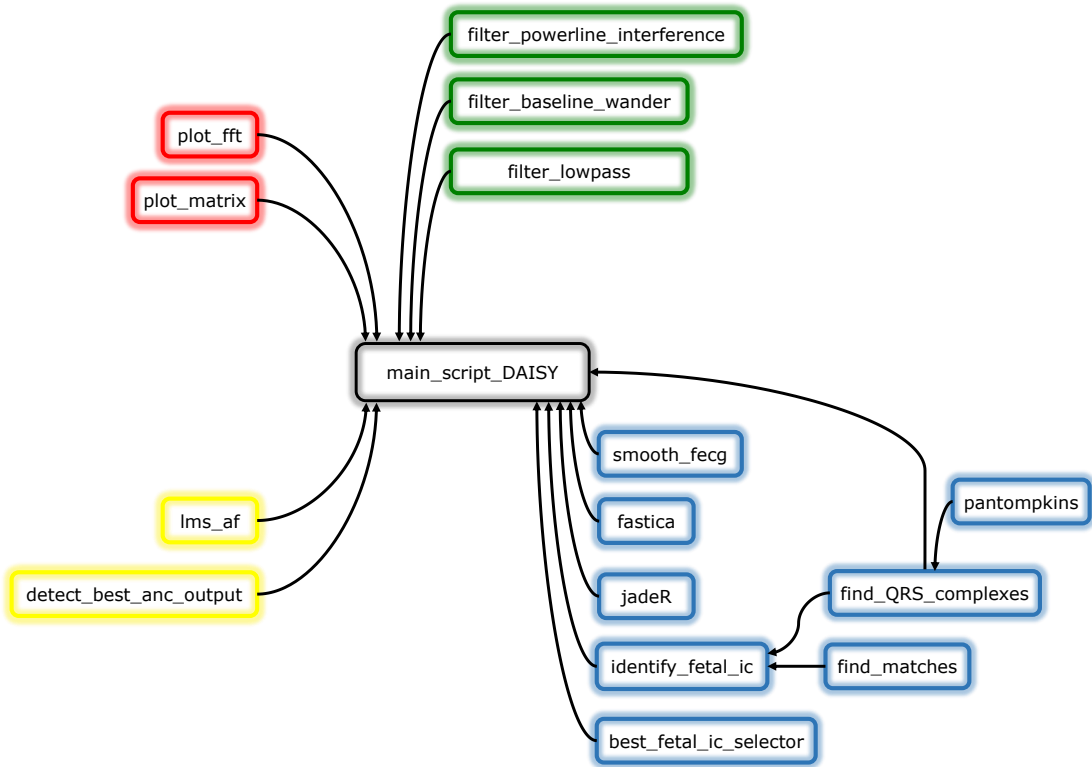


Figure 32: Map of MATLAB functions and scripts for first approach

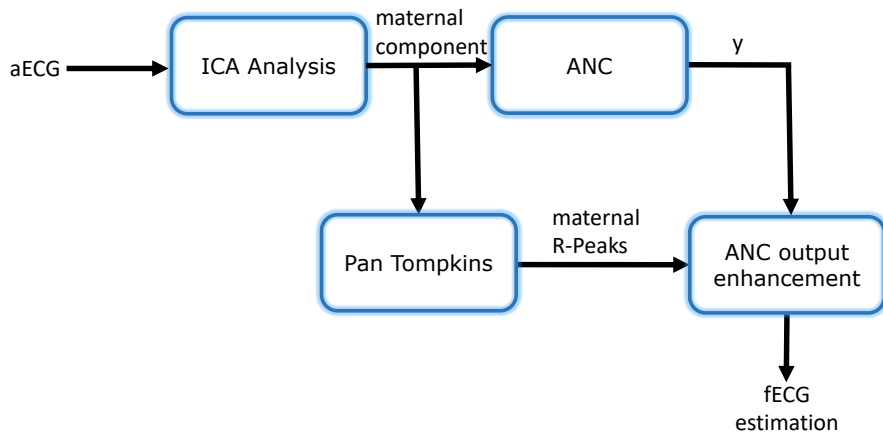


Figure 33: Second Proposed Approach - fECG Extraction Without Using Thoracic Signals

mother and fetus with similar amplitudes for both waves. With the enhancement the maternal R-peaks are almost completely removed and the output signal allows a better identification of the fetal activity.

It can be observed that the second approach produces a set of fetal signals instead of a single signal. This could provide a better view of the fetal cardiac activity as if several leads were available.

2.2.2.2.1 Implementation of the algorithm The second approach was implemented in MATLAB too. In this case one additional function is considered, which is responsible for the enhancement of the ANC output. Figure 34 shows the functions map of the algorithm.

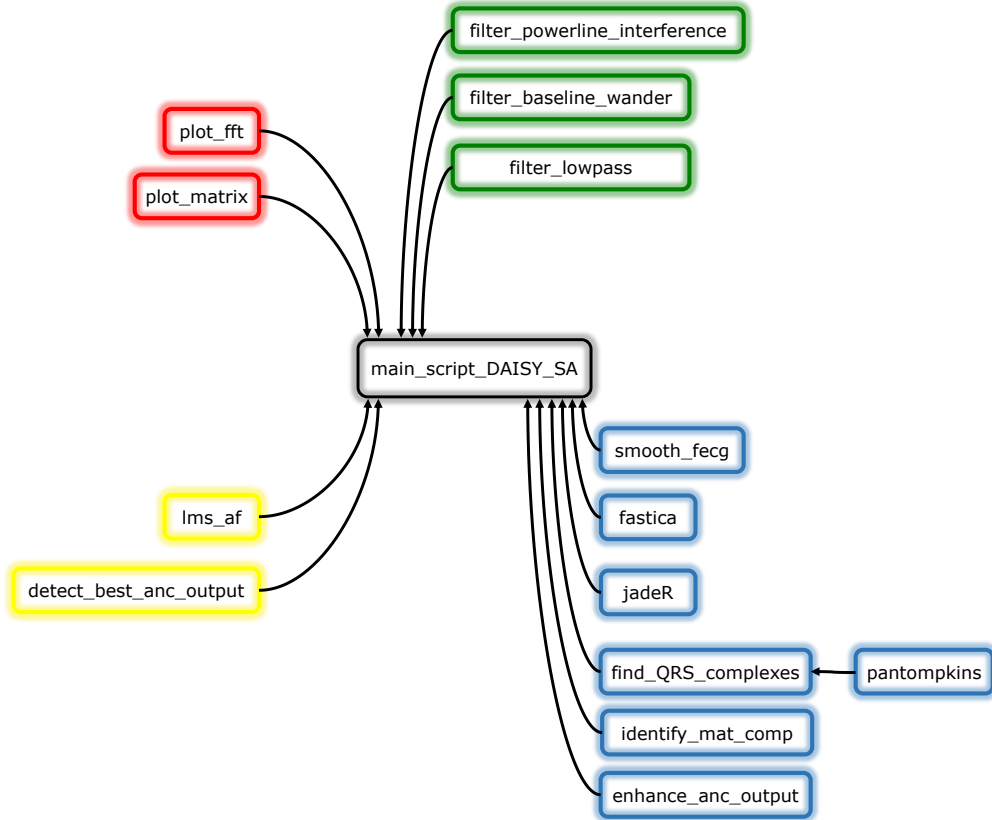


Figure 34: Map of MATLAB functions and scripts for second approach

2.3 Evaluation of the Algorithm

2.3.1 Test Protocol and Metrics to Measure Effectiveness

At this point the effectiveness of the designed algorithm must be tested. To achieve that, a protocol should be designed in order to establish the conditions under which the algorithm is applied on the selected datasets. The selection of the datasets is performed according to the quality of the signals in terms of absence of distortions caused by very strong movement,

measuring errors⁶ or drastic changes in the contact between electrodes and skin. In the case of the DaISy database, because there is only a set of relatively short signals, the whole dataset was considered. For the other two databases specific intervals were selected.

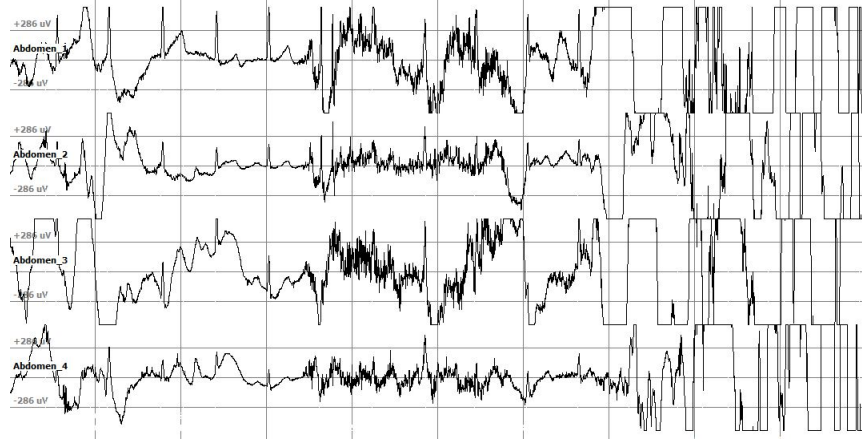


Figure 35: Example of signal interval discarded due to measuring distortion - From database Non-Invasive Fetal Electrocardiogram (Signals were visualized with the tool EDFbrowser)

2.3.1.1 Test Protocol Testing the algorithm is a very important part of the design process as it determines how effective the algorithm is for extracting fECG signals from aECG signals. The general protocol for evaluating the performance of the algorithm is depicted in Figure 36. The protocol could be considered as a white-box conformance test since the code of the algorithm is known [40].

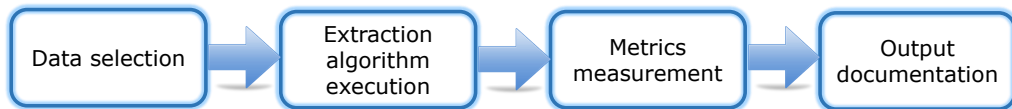


Figure 36: General steps for test protocol

An initial step that becomes relevant is the description of the preparation that is needed for performing the test in terms of hardware and software.

Hardware preparation

General aspects of the machine on which the test is performed include: Microprocessor Core i5, 8 GB RAM, 1 TB HDD. No external hardware is required.

⁶Some signals are strongly distorted due to what seems to be erroneous operation of the measuring equipment. An example of this is provided in Figure 35

Software preparation

General aspects of the software required for executing the test are: MATLAB 2015a. Additional software such as Excel might be used for annotations.

2.3.1.1.1 Data Selection As mentioned before, some of the signals contain a very strong distortion that makes it necessary to discard the intervals during which that distortion appears. Considering this, and also considering that most of the signals have too many samples, some intervals of each signal were selected.

- **DaISy Database** For this database there are both thoracic and abdominal signals but the signals have a small duration (2500 samples). For this reason the whole dataset is considered for the test.
- **Abdominal and Direct Fetal Electrocardiogram Database** For this database a total of 15000 samples per signal are taken. Each dataset has one direct and four abdominal signals. After a visual evaluation of the signals, the intervals with the least amount of noise and abrupt distortion were chosen, as shown in Table 5.

Table 5: Selected data for the Abdominal and Direct Fetal Electrocardiogram Database

Dataset	Selected samples
r01	108600 to 123600
r04	65010 to 80010
r07	155700 to 170700
r08	99150 to 114150
r10	38540 to 53540

- **Non-Invasive Fetal Electrocardiogram Database** This database contains 55 datasets which correspond to recordings taken at different stages of the pregnancy, for a single woman. There are signals from week 22 to week 40 and not every week between that range has a dataset. Instead, for some weeks several datasets built with some days of difference are present. From this database the first 15000 samples of each signal are selected for the test.

From the three databases, it was observed that the Non-Invasive Fetal Electrocardiogram Database has the worst noise conditions while the DaISy database has the best noise conditions.

2.3.1.1.2 Extraction Algorithm Execution After the datasets have been selected, the algorithms are applied on them. This step is the execution of the software programs containing the procedures that make the extraction of the fECG possible.

2.3.1.1.3 Performance Metrics Measurement The selected metrics for measuring the effectiveness of the algorithm are listed below:

- Number of detected fetal R-peaks
- Location of detected fetal R-peaks
- Number of presumable fetal P and T waves

Of course, the fact that there are not known outputs to make a comparison for two of the three databases, some the metrics are subjective. Only for the Abdominal and Direct Fetal Electrocardiogram Database exists a form of comparison because in this case the direct fECG provides the location of the fetal QRS complexes. For the other metrics it becomes hard to determine the accurateness of the detection. However, the repeatability of the waves over time and they appearance should give a certain degree of certainty to the detection.

2.4 Comparison With Other Algorithms

2.4.1 Compared Methods

The selection of the methods for the comparison was made according to the information obtained in the review of the most relevant techniques (See subsection 1.2) and also according to the methods that were combined in the proposed approaches. Because the methods were combined, it becomes interesting to test how the performance of the individual methods may be improved when they are combined. Following this idea, the methods that were compared to the developed methods are

- Independent Component Analysis (FastICA and JADE algorithms)
- Adaptive filters (LMS-based Adaptive Noise Canceller)

2.4.2 Comparison Test

The comparison test is applied on the datasets for which the proposed algorithm was tested previously. The same metrics of effectiveness described for the test of the proposed algorithm are used for the comparison. One particularity of the comparison is the fact that for the case of the Abdominal and Direct Fetal Electrocardiogram Database there are no thoracic signals available, meaning that there is no reference signal for the test of the ANC. For this reason, only ICA is tested on this database. For the two other databases both ICA and adaptive filters are tested.

3 RESULTS

This section of the document presents the results of the executed tests and their corresponding analysis. The proposed approaches described in previous section were applied on the three databases for the selected data.

3.1 Results of First Approach

Because the first approach requires thoracic signals, this approach cannot be applied on the Abdominal and Direct Fetal Electrocardiogram Database. For the two remaining databases the results for the first approach are now presented.

3.1.1 First Approach - Results on the Non-Invasive Fetal Electrocardiogram Database

Due to the fact that the first approach depends on the effectiveness of ICA for extracting a fetal component, this approach does not provide good results on this database because of the very low SNR of the fECG. Figure 37 shows an example of the components extracted with the FastICA algorithm for the dataset *ecgca473*. The same can be said about the ANC, whose output does not contain a fetal signal without maternal activity. For these reasons, the first approach is not a suited method for extracting the fECG from the Non-Invasive Fetal Electrocardiogram Database. All datasets were tested and for none of them a fetal signal could be extracted.

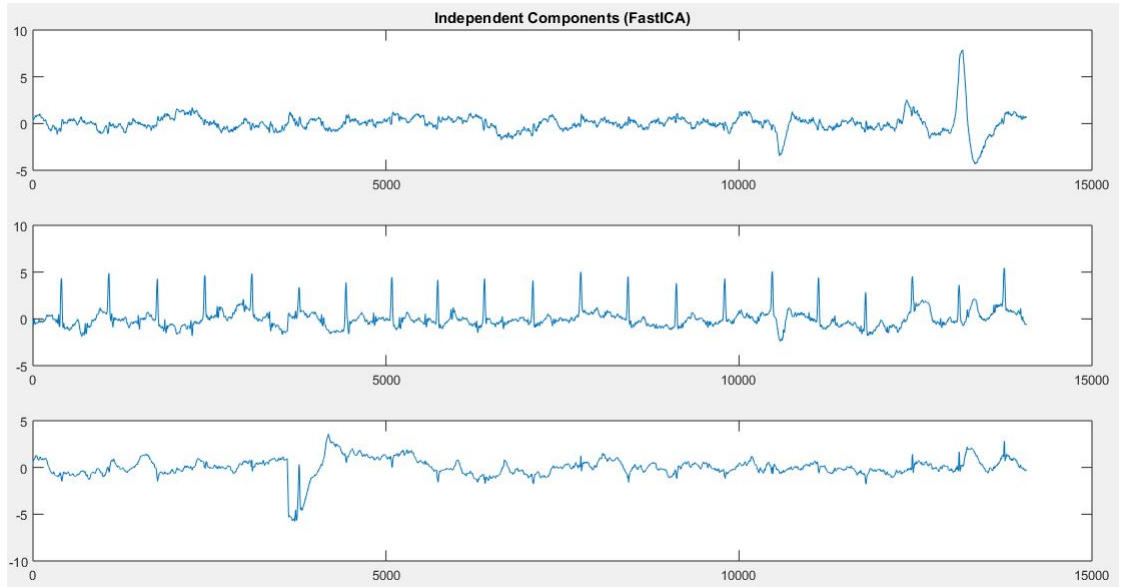


Figure 37: Independent components after FastICA algorithm on Non-Invasive Fetal Electrocardiogram Database, dataset *ecgca473* - First Approach

3.1.2 First Approach - Results on the DaISy Database

This database contains only one set of signals that corresponds to a pregnant woman. It also contains the best quality among the used databases in terms of low noise and high amplitude of the fECG.

This approach, as explained before, uses both thoracic and abdominal signals to produce an estimation of the fECG signal. The algorithm was executed on the signals and the abdominal signals after the filtering stage are shown in Figure 38. The output of the ANC block is shown in Figure 39. One of these signals is selected as output for the fECG estimation; in this case the first signal is the most prominent fetal signal. The independent components obtained by the JADE algorithm are shown in Figure 40. As explained in the description of the first approach, the fetal components of the output of the FastICA and the JADE algorithms are compared and one of them is selected for further analysis. In the case of the DaISy database the JADE fetal component is selected. Then, at the fECG generator a new signal that contains the information of both the ANC block output and the ICA Analysis block is produced. The resulting fECG signal is shown in Figure 41.

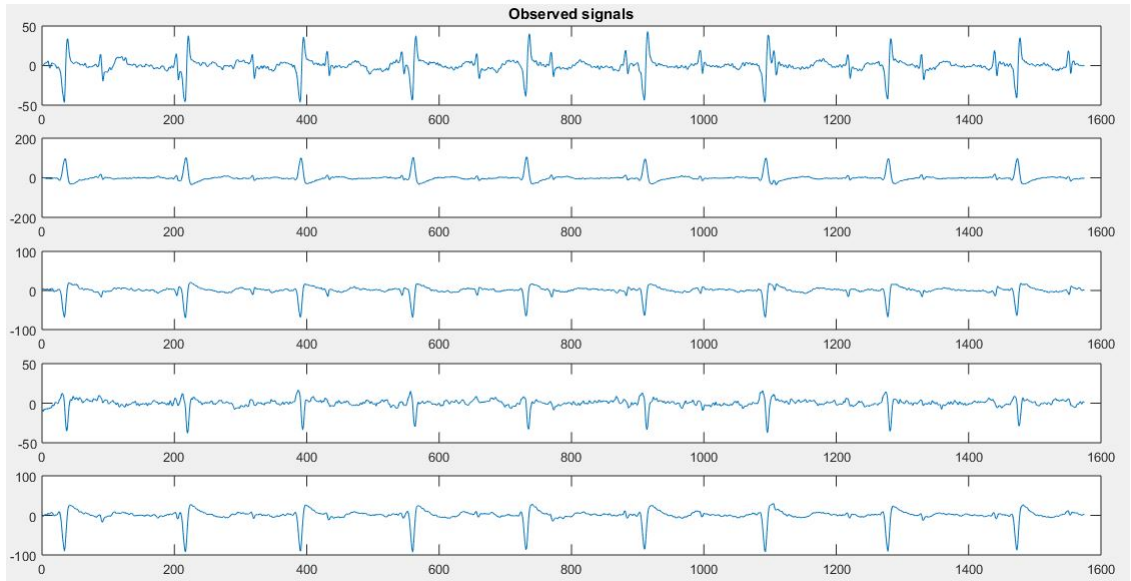


Figure 38: Abdominal signals after pre-processing stage on DaISy Database - First Approach

Although it is hard to classify an amplitude variation as T-wave when there is no desired output for comparison, the pattern of repetition and the type of variation should give an idea about which variations may correspond to a T or P wave. The resulting signal contains some variations that could be due to the T and P waves of the fECG. If the signals of the database had a higher length it would be easier to analyze the pattern of repetition of the variations and also the waveform to increase the certainty of the classification as T or P waves. A total of 5 and 3 presumable T and P waves, respectively, can be observed in the fetal signal.

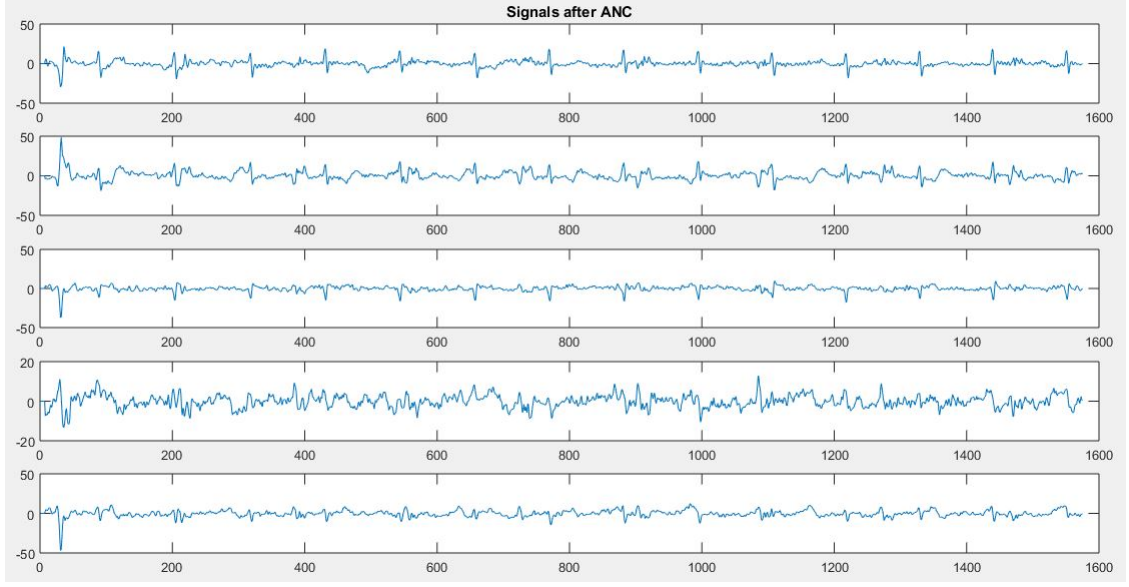


Figure 39: Signals after ANC on DaISy Database - First Approach. First signal corresponds to the fetal signal selected for further analysis

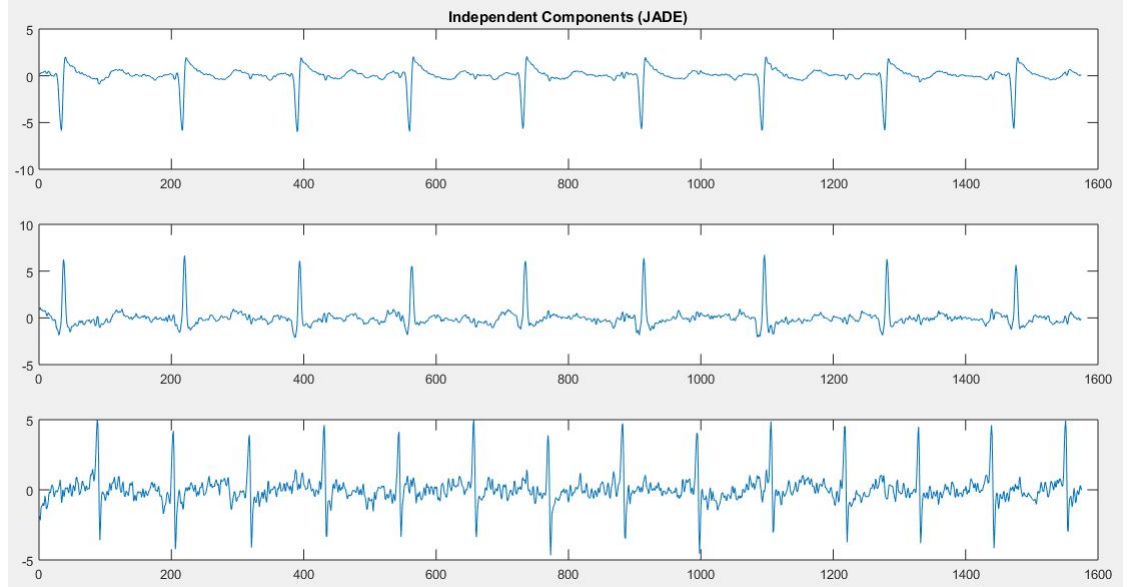


Figure 40: Independent components obtained with JADE algorithm on DaISy Database - First Approach. Component of the bottom corresponds to the fetal signal selected for further analysis

The Pan-Tompkins algorithm can be easily applied to the resulting fetal signal to find the locations of the fetal R-peaks. With this locations the time intervals between consecutive R waves can be determined, their mean can be obtained, and the fHR can be then computed by using the formula $60/\text{meanRR}$, where meanRR is in seconds. Following this procedure,

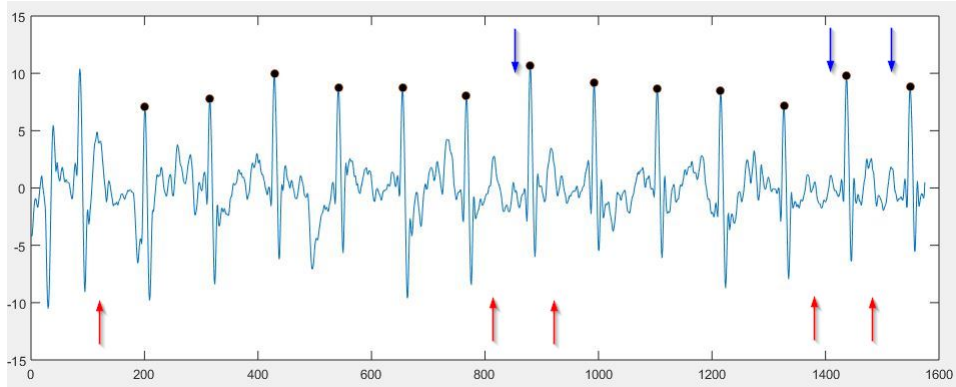


Figure 41: fECG signal obtained on DaISy Database with the first approach. Red arrows denote the presumable fetal T waves and blue arrows denote the presumable fetal P waves. Black dots show the fetal R-peaks identified through the Pan-Tompkins algorithm

the fHR has a value of 133.54 bpm.

3.2 Results of Second Approach

This approach does not require thoracic signals. For this reason, it could be tested on all three databases. As explained before, this approach produces as many fetal signals as abdominal signals available. Some of these fetal signals will be a better representation of the fECG depending on the quality of the measurement and also on the position of the recording electrode. Therefore, one of these signals should be selected for the measurement of the parameters that will provide information about the condition of the fetus. The signal that is most suited for the extraction of the parameters is selected visually. The reason for doing it this way is that some of the signals will be similar and also some of them will be expected to provide more information about the morphology of the fECG.

3.2.1 Second Approach - Results on the Abdominal and Direct Fetal Electrocardiogram Database

This database contains 5 datasets. Each dataset corresponds to a different woman. The gestation time is between the 38th and the 41st week, which should imply somehow that the fetal signal has reached an appropriate amplitude for the extraction. After the second approach was applied on the datasets, as mentioned before, there are as many fetal representations as there are abdominal signals. An example of this is shown in Figure 42 for the dataset *r08*, in which it can be observed that the last signal has the highest amplitude and would be thus the most appropriate signal for extracting parameters such as fHR.

From Figure 42 it can be also observed that some fetal R-peaks are missing around samples 5000, 7300 and 8700. The missing fetal R-peaks are due to the overlap between fetal and maternal peaks. Because of how the approach works, when that overlap occurs, the fetal peak is removed because the complete maternal peak is removed during the enhancement of the ANC's output. However, the remaining fetal R-peaks should be enough to provide a good

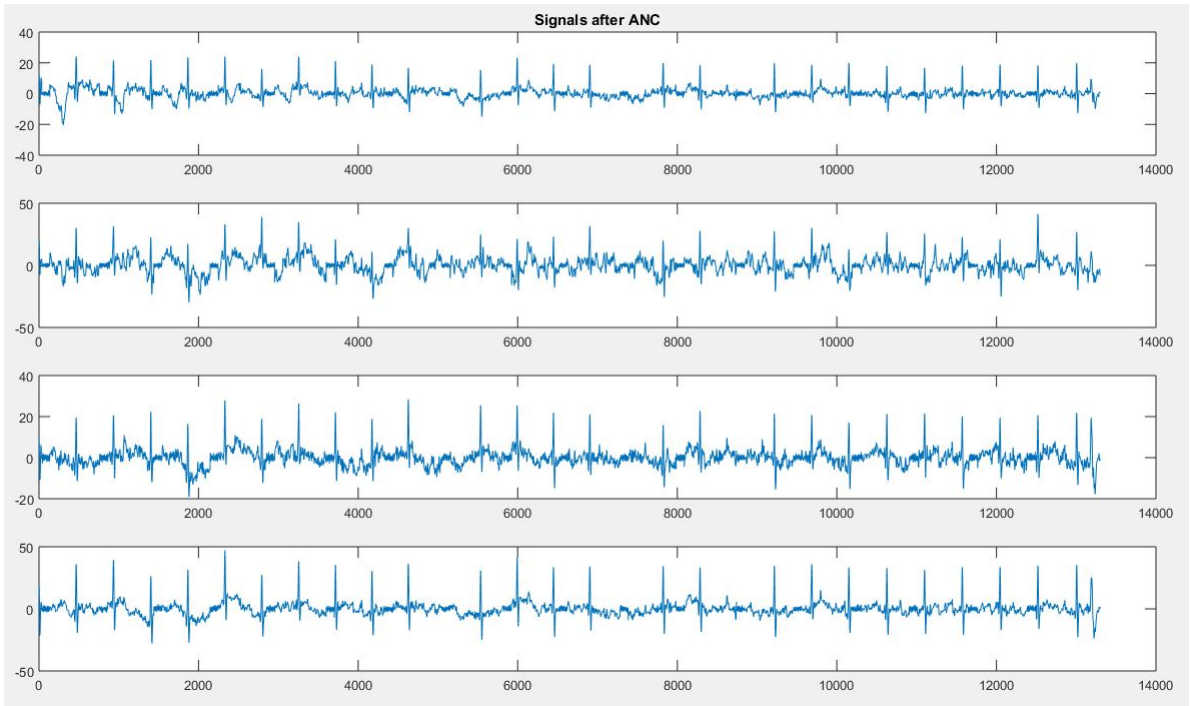


Figure 42: fECG signals obtained on Abdominal and Direct Fetal Electrocardiogram Database (dataset r08) - Second Approach

representation of the fHR.

Figure 43 shows the best fetal signals for each dataset in the database. The best signal was selected visually according to the amount of noise and the amplitude of the signals obtained at the output of the enhancement block.

Unlike the first approach, in this case the possibility of extracting T waves is smaller due to the fact that ICA is not able to separate the fetal signal from the abdominal signals and also due to the absence of thoracic signals. The T waves that appear in the extracted fetal signals come from the maternal cardiac activity.

One advantage of this database is the fact that the direct fetal electrocardiogram is available. This allows a comparison between the real R-peaks and those peaks found in the extracted signals, for each dataset. Table 6 shows the results of a comparison between the R-peaks from the direct measurements and those from the signals obtained through the second approach. For the comparison only the correctly identified fetal R-peaks are compared to the fetal R-peaks specified in the annotations of the database, which means that the real peaks for which there are no identified peaks in the output signal are discarded. For the detection of the fetal R-peaks the Pan-Tompkins algorithm is employed. This algorithm allowed the correct detection on the datasets r10, r08 and r01. For datasets r07 and r04, given the high amount of noise, a visual examination was performed in order to identify the fetal R-peaks

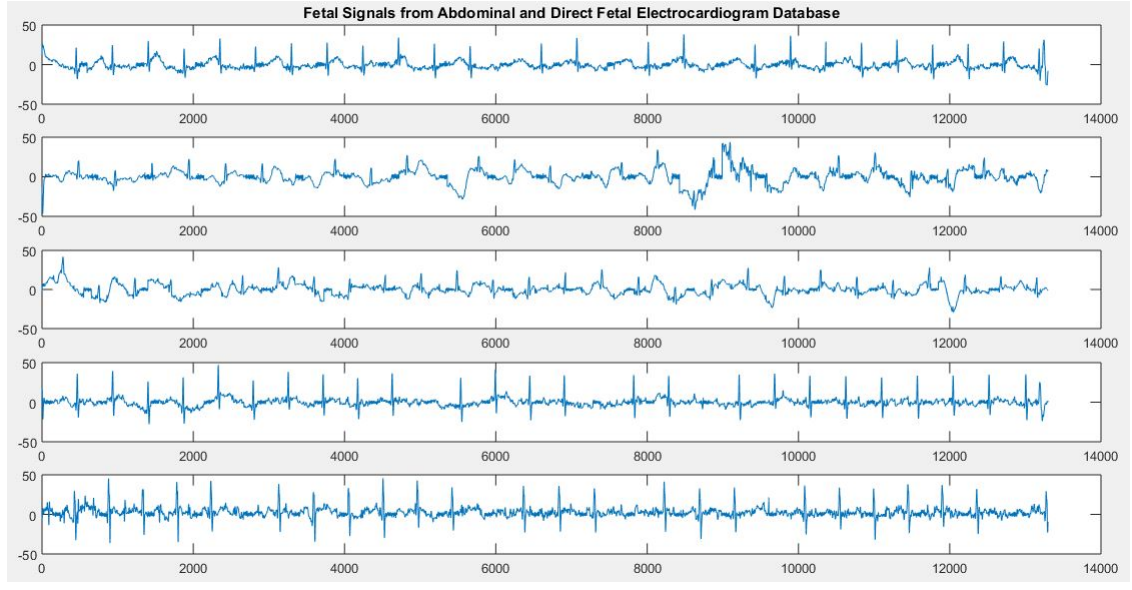


Figure 43: fECG signals obtained on Abdominal and Direct Fetal Electrocardiogram Database (all datasets) - Second Approach. From top to bottom the datasets are: r01, r04, r07, r08 and r10

that could not be detected with the mentioned algorithm.

The mean square error (MSE) is used to compare the deviation of the real and the obtained peaks (in terms of time locations) according to expression 14, in which \hat{Y} is a vector with N predictions and Y is a vector with N real values. The time intervals between consecutive detected fetal R-peaks are also compared through the MSE. This interval comparison becomes an important tool for comparing the found peaks, because possible small delays caused during the processing stage will have no effect on the MSE (because the delay would affect all the instants equally given the type of processing techniques implemented). Delays could be also due to changes in the morphology of the fetal QRS complexes. The units of the MSE are, for both cases shown in Table 6, samples².

$$mse = \frac{1}{N} \sum_{i=1}^N (\hat{Y}_i - Y_i)^2 \quad (14)$$

Table 6: Comparison between R-peak locations and intervals on the Abdominal and Direct Fetal Electrocardiogram Database

Dataset	Number of found R-peaks	MSE Locations	MSE Intervals
r01	24/28	4.0417	1.4348
r04	20/27	51.100	4.6316
r07	24/28	59.8750	5.4783
r08	24/29	4.7083	0.3043
		➡	

Table 6

Dataset	Number of found R-peaks	MSE Locations	MSE Intervals
r10	23/29	11.2174	11.4545

3.2.2 Second Approach - Results on the Non-Invasive Fetal Electrocardiogram Database

This database offers the worst noise conditions among the tested databases. The fECG has also a very low amplitude. This can be appreciated in the abdominal signals, in which fetal peaks can be barely noticed visually. Although the ICA algorithm is capable of extracting a component with almost only maternal activity, the ANC and the enhancement of its output are not effective enough to produce a fetal signal that can be used for extracting parameters such as the fHR. A signal obtained after the enhancement is shown in Figure 44 for dataset *ecgca840*. For the other datasets the approach was tested too and the results are similar: for none of the output signals a clear fetal signal could be obtained.

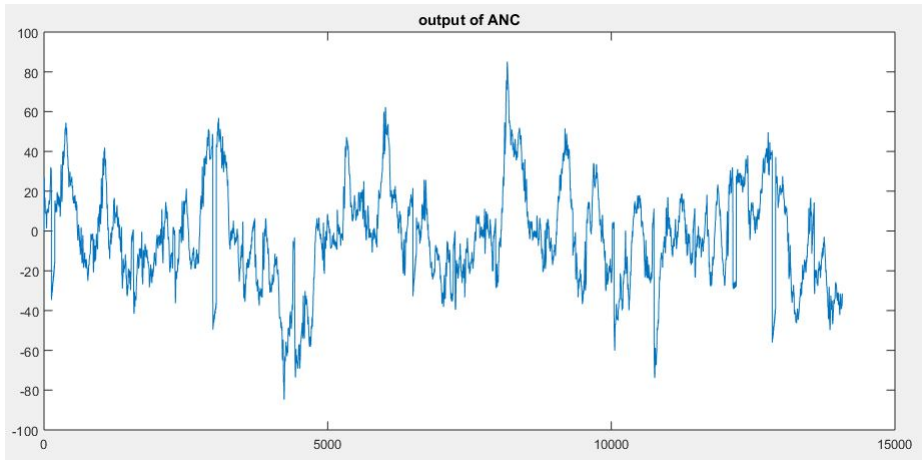


Figure 44: Output signal on Non-Invasive Fetal Electrocardiogram Database, dataset *ecgca840* - Second Approach

3.2.3 Second Approach - Results on the DaISy Database

The second approach was applied on the DaISy database in order to test the performance if no thoracic signal were available. The resulting signal (Figure 45) contains more noise than the independent component extracted through the ICA algorithms. In the figure the fetal R-peaks detected with the Pan-Tompkins algorithm are shown as black dots. The fHR can be calculated from the detected R-peaks, resulting in 133.29 bpm, which is very close to the heart rate obtained using the component extracted by ICA (133.53 bpm - Reported in next subsection).

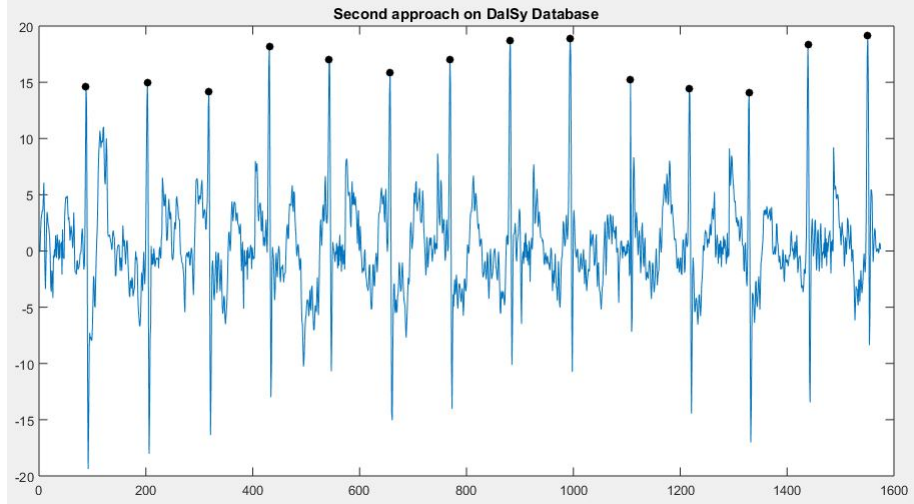


Figure 45: fECG signal obtained on DaISy Database - Second Approach

3.3 Comparison Test

The comparison test was executed using the same datasets used previously for the proposed approaches. The same pre-processing procedures applied before are applied in this case. If no fetal component is clearly observed in the extracted independent components, then all of them are shown. If a fetal component is easily observed, then only this signal is presented.

3.3.1 Results of ICA

3.3.1.1 ICA - Results on the Abdominal and Direct Fetal Electrocardiogram Database For this database the ICA technique does not allow the extraction of a fetal component. The method was tested on each of the 5 datasets and the results were the same: all the independent components contain both maternal and fetal activity. Figure 46 shows the obtained ICs for the dataset *r10*.

3.3.1.2 ICA - Results on the Non-Invasive Fetal Electrocardiogram Database As stated before, this database has the lowest signal quality. The signals contain a high amount of noise that makes the ICA algorithms incapable of extracting a fetal component. As Figure 47 shows, only the second extracted component represents a clear ECG signal, but this signal describes mostly maternal activity. This components are for the dataset *ecgca473* whose signals were taken during the last stages of the pregnancy (week 39). The fetal component should be stronger in the signals of this gestation time in comparison to signals taken previously. For the remaining datasets the results are very similar, with no fetal signal being extracted.

3.3.1.3 ICA - Results on the DaISy Database Both the FastICA and the JADE algorithms were tested on this database. The fetal components for the two algorithms are very similar. Figure 48 shows the fetal component obtained by the FastICA algorithm, with the

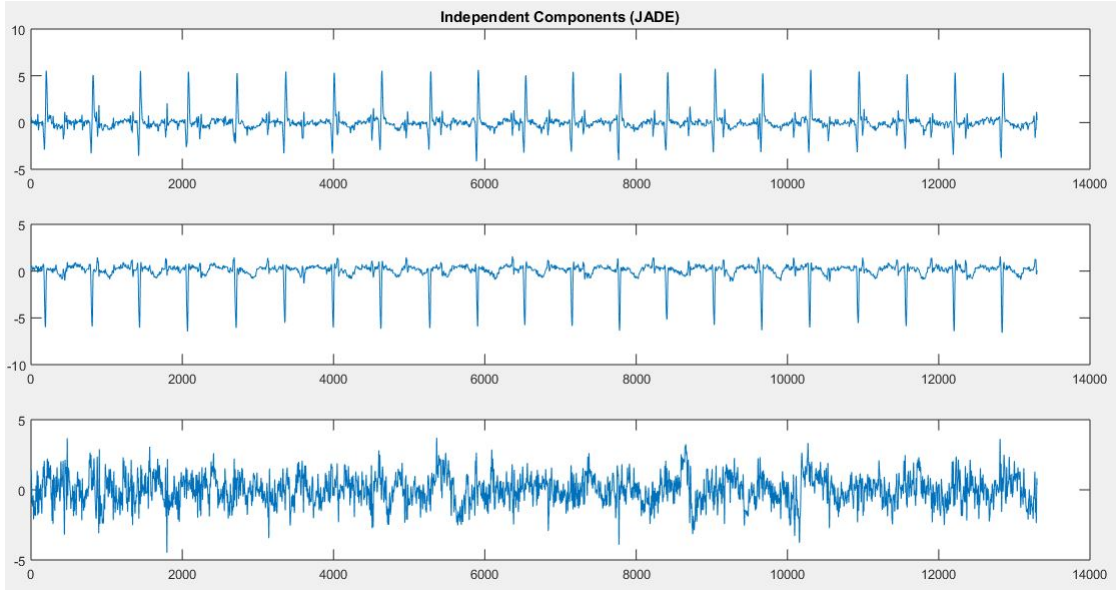


Figure 46: Independent components obtained with the JADE algorithm on the Abdominal and Direct Fetal Electrocardiogram Database. No fetal component can be observed

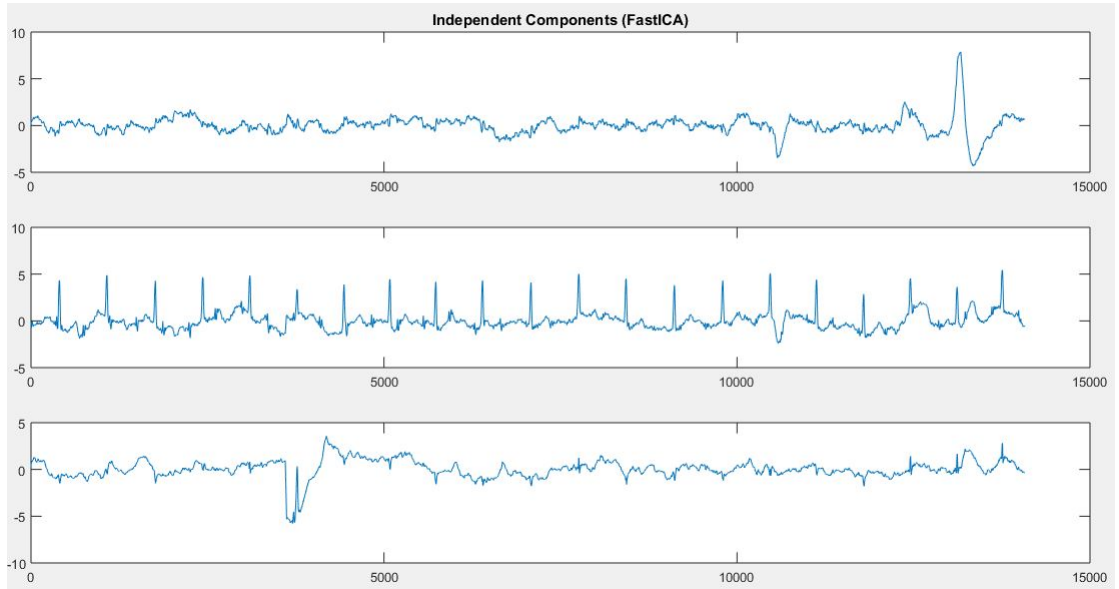


Figure 47: Independent components obtained with the FastICA algorithm on the Non-Invasive Fetal Electrocardiogram Database. No fetal component can be observed

fetal R-peaks as black dots. This is the only database for which the ICA algorithms allowed a good extraction of the fetal component.

The fHR can be calculated, as done previously, from the RR intervals. The fHR is 133.29

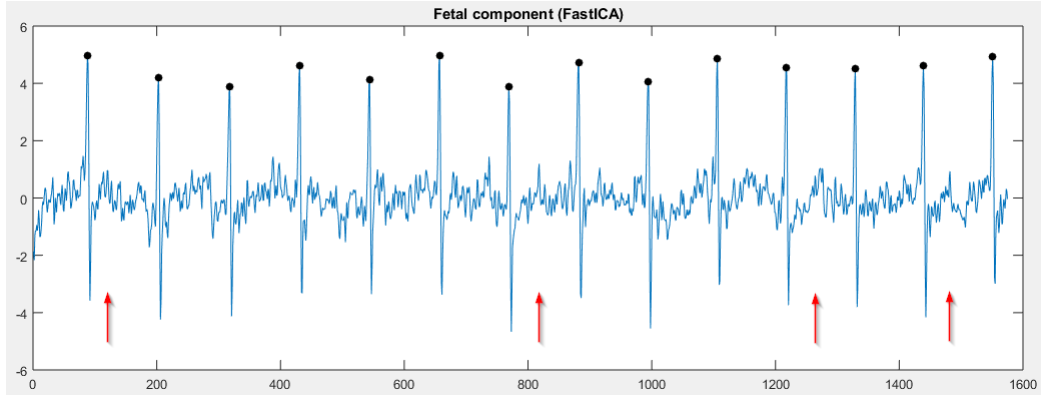


Figure 48: Fetal component obtained with the FastICA algorithm on the DaISy Database. Red arrows point to variations that could correspond to T waves

bpm, which is close to the HR obtained for the first proposed approach. The Pan-Tompkins algorithm detected one additional peak (the first one) as compared to the case of the first approach. If this peak is not considered for the computation of the fHR, then the result is 133.53, which is much closer to the result for the proposed approach.

From the signal shown in Figure 48 the fetal R-peaks can be easily identified. However, in the case of the presumable T waves it becomes hard to establish whether a variation after an R-peak corresponds to a T wave or not. This is caused mainly due to the low SNR of the fetal signal. Some of the variations between R-peaks could be assumed to correspond to possible T waves. However, these variations (red arrows in Figure 48) do not show a clear waveform and would be thus not suited for being considered in a morphological analysis.

3.3.2 Results of Adaptive Filter

As explained before, only two of the three databases contain thoracic signals. Because the ANC needs a reference signal, this method cannot be tested on the Abdominal and Direct Fetal Electrocardiogram Database. Another important factor to highlight is that while ICA provides (ideally) one single signal that corresponds to the fECG, the adaptive filters are applied on each abdominal signal, generating therefore several possible representations of the fetal activity. Thus, the signal with the most evident fetal activity was chosen for reporting the results.

3.3.2.1 Adaptive Filter - Results on the Non-Invasive Fetal Electrocardiogram Database In the case of this database, because of the very low SNR, the ANC is barely capable of reducing the maternal peaks. The dataset *ecgca473* was used. The very low amplitude in the fetal heartbeats makes it impossible to recognize any fetal activity. Figure 49 present the signals produced by the ANC. Different parameters such as filter length and rate of convergence were tested. High filter lengths showed a better removal of the maternal activity but at the same time higher removal of the fetal peaks. Low filter lengths showed the opposite situation. This behavior was better appreciated on the DaISy database, for which

the length was heuristically adjusted to produce the best representation of the fetal signal. For this reason, the filter length and rate of convergence should be selected properly for a better performance of the ANC. In regard to this database, the adjustments of the adaptive filter parameters did not bring any considerable improvement of the output signals for any of the datasets.

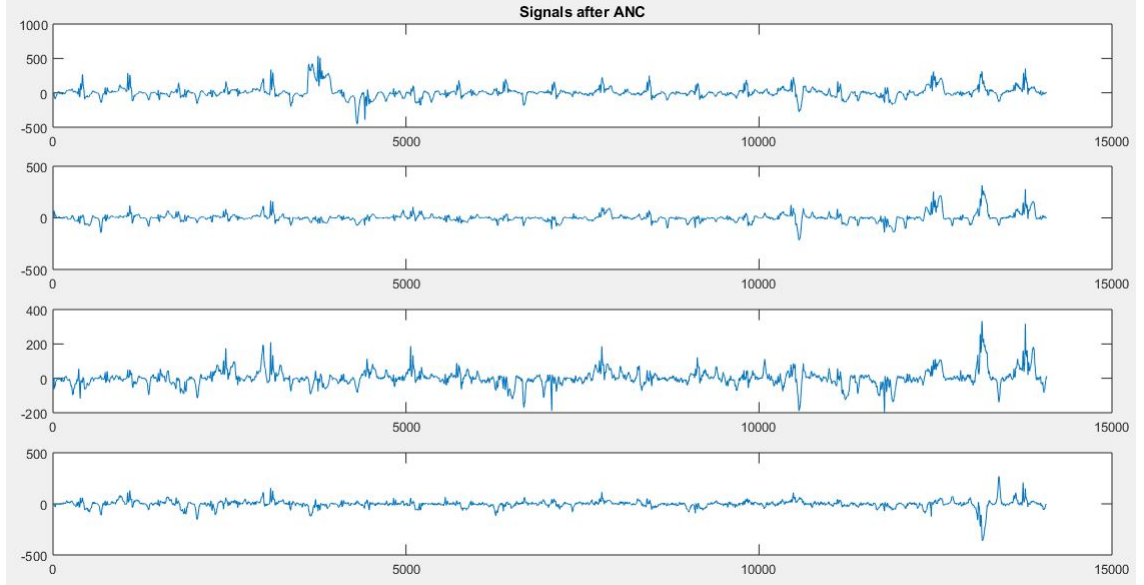


Figure 49: Filtered abdominal signals obtained with the ANC on the Non-Invasive Fetal Electrocardiogram Database. None of the signals show fetal activity clearly

3.3.2.2 Adaptive Filter - Results on the DaISy Database The LMS-based ANC was tested on the DaISy database, using one of the thoracic signals as reference. Each of the abdominal signals was filtered in order to reduce the effect of the maternal component. Figure 50 shows the resulting signals. It can be observed that the first and the third signals are the ones with the best morphology for the extraction, for instance, of the fHR.

The first signal is the most suited for finding the fHR because the fetal R-peaks have the highest amplitude. Again, the Pan-Tompkins algorithm leads to the R peaks and the heart rate is computed. The result is 133.10 bpm. This signal, like in the case of ICA, shows some variations that could be thought to correspond to T waves (Figure 51).

3.4 Analysis of Results

3.4.1 First Approach

In the first approach, the best results were obtained on the DaISy database. For this database the fetal R-peaks can be easily recognized. Some presumable P and T waves can be observed too. The fetal R-peaks lead to a HR that is consistent with the normal HR for fetuses. One important aspect of the method is that the fetal R-peaks can be identified even when there

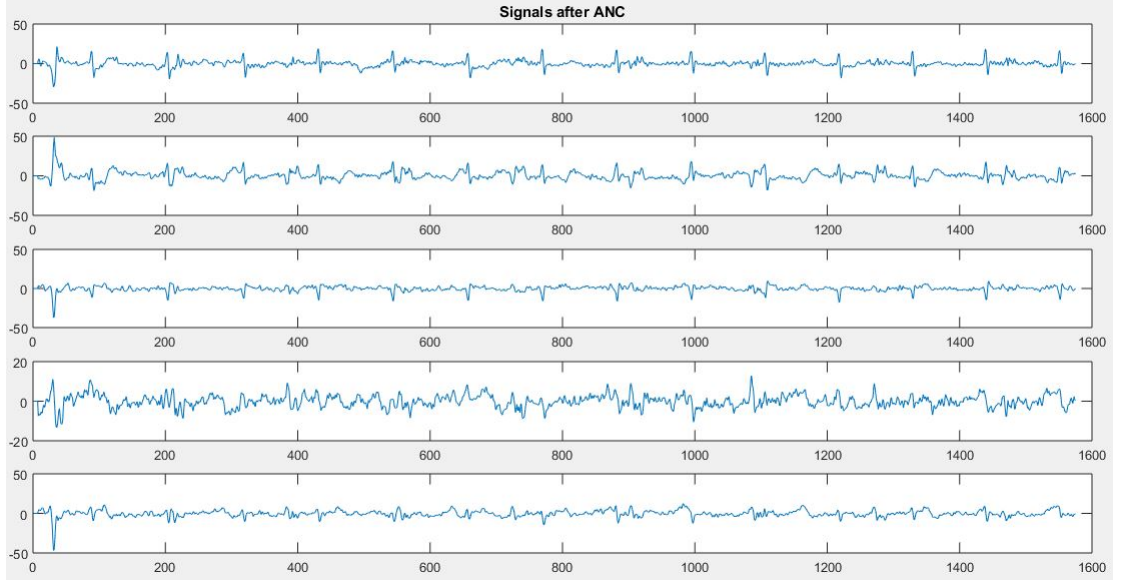


Figure 50: Filtered abdominal signals obtained with the ANC on the DaISy Database. First and third signals are the best representations of the fetal activity

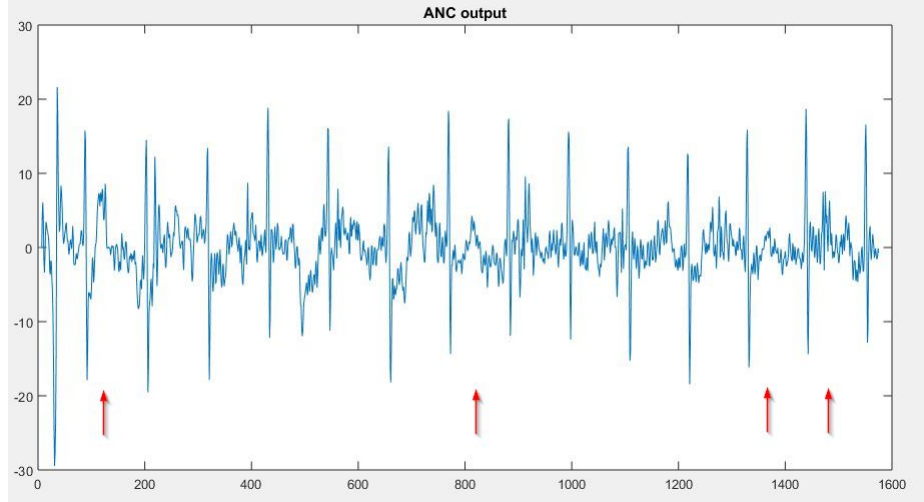


Figure 51: Most prominent signal from ANC on the DaISy Database. Red arrows point to possible T-wave-related variations

is an overlap between maternal and fetal R-peaks. This overlap happens partly for the first abdominal signal between samples 1000 and 1200 (See Figure 38). This is an important feature of the method because the less fetal information is missed by an extraction method, the more information would be available for an eventual diagnosis. The use of the Pan-Tompkins algorithm applied to fetal signals was also important for the detection of the fetal QRS complexes. Because thoracic signals are available for this database (and thus the locations of

the maternal R-peaks), the Pan-Tompkins algorithm was modified so that it could ignore the R-peaks that would probably not correspond to fetal activity, based also on the locations of next and previous fetal R-peaks. This improves the method given the fact that the ANC requires a certain amount of time to modify the filter coefficients and can therefore let some maternal peaks remain after the filtering process.

The P and T waves found on the DaISy database can be only presumed to belong to the fetus because there is no known fetal signal for a comparison. However, the pattern of occurrence and waveform suggest that they do not represent maternal waves or noise. Because of the noise that remains after the filtering stage and the separation techniques and, because the dataset of the DaISy database is very short (2500 samples, sampling frequency of 250 Hz) in comparison to the datasets of the other databases, the certainty of the found T and P waves becomes harder to establish. Longer signals with the quality of this database would have given a better chance to analyze the pattern of repetition and the similarity among the presumable T and P waves. The intermittent occurrence of these waves shows the effect that the noise may have on the output signal, justifying therefore a well designed pre-processing stage.

The results of the first approach on the Non-Invasive Fetal Electrocardiogram Database show how the first approach depends on the effectiveness of the extraction of components performed by the ICA algorithms and also on the implemented adaptive filter. Regarding ICA, the very low SNR of the fECG for this database limits the extraction. The independent components provided by ICA include some maternal activity. The second component shown previously for the FastICA algorithm (Figure 37) shows a signal that combines the activity of both mother and fetus, showing the limitation of the separation when the SNR of the fECG does not reach suited values. The ANC is also incapable of extracting a fetal signal for each abdominal signal because of the distortion of the abdominal signals with respect to the thoracic signals. The noise that distorts the abdominal signals sets hard conditions for the ANC, which modifies the filter coefficients trying to produce an output that does not contain maternal activity. Unfortunately, unlike the case of the DaISy database, the output still contains more maternal activity than fetal activity.

3.4.2 Second Approach

With the second approach no thoracic signals are required. This method is therefore more appropriate for processing the datasets of the Abdominal and Direct Fetal Electrocardiogram Database, for which only abdominal and direct signals are available. Because there is a direct measurement for each dataset with almost only fetal activity, the found R-peaks could be compared in order to establish if the found locations corresponded to the peaks of the direct recording. The test executed for all five datasets showed that in all cases most of the fetal R-peaks can be either automatically or visually identified. The peaks that could not be identified are those that overlap with the maternal R-peaks. Table 6 presents the information about the comparison with the direct measurements. In all cases, more than 70 % of the fetal R-peaks could be identified. This number obviously depends on how many times there is an overlap between maternal and fetal R-peaks. Determining the fHR and fHR variability is possible, however, if some of the fetal R-peaks are missing. This is because those parameters are based

on the time intervals between consecutive intervals instead of on the amount of peaks. For a higher precision on those parameters, the number of peaks can be increased by increasing the number of samples analyzed. The computed MSE resulted to be higher for those signals with a higher amount of noise and lower amplitude of the fetal component. The MSE for the intervals are more consistent with the intervals of the direct measurement, showing that a change on the waveform could be occurring (which may be expected given that the direct signal is measured on the fetal scalp), causing thus the maximum value of the peaks to delay a few samples.

The test for the Non-Invasive Fetal Electrocardiogram Database did not bring the expected results, mainly due to the same problem that sets a limit for ICA, namely the very low SNR of the fECG. Although the ICA produces a good estimation of the maternal component that can be used in the ANC, the variations of the abdominal signals caused by noise that could not be removed during the pre-processing stage cause the ANC signal to have abrupt changes after its enhancement. Considering the changes caused by the noise, the output signal is not “clean” enough to allow an automatic or even visual identification of the fetal R-peaks.

Finally, the second approach was effective for extracting the fetal R-peaks from the abdominal signals. All of the R-peaks were correctly extracted and the computed fHR was consistent with the fHR computed on the fetal component produced by ICA and also with the fHR computed for the output obtained from the first approach.

3.4.3 Comparison

The comparison test was useful for establishing how effective the individual methods (ICA and adaptive filters) are in comparison to the proposed combined approaches. In the case of ICA, it was capable of extracting a fetal component only for the DaISy database. The extracted fetal component contains easily distinguishable R-peaks, but it does not contain easily identifiable presumable T or P waves as compared to the signal obtained for the first approach. For the other two databases the technique is not capable of extracting an independent fetal component. This is due mainly to the low SNR of the fECG but there could also be cases for which the location of the measuring electrodes are not correctly distributed, causing two signals to be too similar, providing almost the same information. This would be equivalent to locating two microphones at the same location in the cocktail party example explained previously for ICA.

The adaptive filter could be applied on two databases only, due to the requirement of thoracic signals that can be used as reference. Regarding this databases, the results show good performance on the DaISy database. The resulting signals represent mostly fetal activity. One of these signals can be used to determine the fHR. Some variations that could correspond to fetal T waves were observed too.

When tested on the Non-Invasive Fetal Electrocardiogram Database the adaptive filter was not capable of removing the maternal activity completely. Therefore, the processed abdominal signals still contain more maternal activity than fetal activity.

4 CONCLUSIONS AND FUTURE WORK

4.1 Conclusions

In this work an algorithm for the non-invasive extraction of the fetal electrocardiogram from abdominal recordings was presented. The algorithm is divided into two approaches: The first approach uses both abdominal and thoracic signals and the second approach uses abdominal signals only. Both approaches are implemented with a combination of Independent Component Analysis and Adaptive Noise Cancellation.

Regarding the pre-processing stage, the polynomial fitting for the removal of the baseline wander was modified in terms of the knots that are used for the fitting of the polynomial. The Q and S peaks were used instead of the PQ interval. This modification showed to be effective when all peaks could be detected by the Pan-Tompkins algorithm. Because all peaks cannot be always determined by the algorithm due to different factors such as noise, artifacts and abrupt distortions, considering the conventional LTI-FIR filter in those cases was an effective strategy for baseline removal.

The three blocks that conform the first approach were aimed to the automation of the extraction process and the selection of the best output according to different criteria. In the case of the ICA analysis block, the selection of the fetal component is performed automatically based on the peaks detected by the Pan-Tompkins algorithm. This helps to compensate the “random” order of the components generated by ICA and brings the advantage of not depending on a visual inspection of all components for each ICA algorithm considered. After the fetal component has been identified for each ICA algorithm, the best component is selected. This selection was implemented with a matched filter that allows the identification of the signal with the cardiac cycles that are most similar to a common cardiac cycle (containing all standard waves P, QRS complex and T). Because different ICA algorithms will provide different fetal components, the selection of the one that contributes with most morphological information becomes an advantage for the method. Another advantage of the method and, particularly, of the way the ICA block was implemented, is that more ICA algorithms can be easily added. For the ANC a similar consideration was made. Because there are several signals at its output, the selection of the most prominent fetal signal is an important step that was implemented automatically. The selection of the length of the FIR filter of the ANC and the rate of convergence was relevant for obtaining output signals with a considerable reduction of the maternal activity. Finally, the fECG generator block considers the common changes in the signals obtained from ICA and from the ANC. This helps to produce a fetal signal that considers the morphology contributions of both signals, being therefore focused on the morphology.

Results for the first approach helped to show the requirements that it has for an appropriate performance: The SNR of the fECG must meet the requirements of SNR that both ICA and the ANC need in order to produce signals that correspond only to the fetal activity. The DaISy database was, among the two databases tested in this approach, the only one that

offered those SNR conditions, leading to the best results. When these conditions are met, parameters such as the fHR can be extracted from the resulting signal either automatically or through visual inspection. Other parameters such as the ST segment could be also analyzed but a longer signal would be necessary to ensure that those signals correspond to the fetal activity. For the obtained result, however, the pattern of repetition and shape of the presumable T and P waves suggest that they actually correspond to the fECG. This result could also be improved by implementing more complex and advanced pre-processing techniques.

The Non-Invasive Fetal Electrocardiogram database has two main disadvantages that should be remarked: (1) The level of noise and artifacts present in the signals of this database is considerably high, and (2) The fact that the database corresponds to measurements performed on a single woman implies that there is no possibility of having different types of fECG morphologies. The first disadvantage could not be completely avoided with the implemented pre-processing techniques and more advanced techniques might be required to solve this issue. Some fluctuations of the signals that seemed to correspond to baseline wander could not be removed. There were therefore important variations in the processed signals that might have affected the result. Regarding the second mentioned disadvantage, the fetal peaks are barely recognizable among the noise. Measurements taken from different women could provide fetal signals with possibly better amplitudes and waveform patterns that could have been enough for having a higher SNR, allowing thus ICA and the ANC to generate better fECG representations. Modern measurement equipment and analogue pre-processing techniques should help to overcome the problems that this database has in terms of noise and artifacts.

The results for the second approach show that this algorithm is suited for extracting the fetal R-peaks under normal noise conditions such as the conditions of the DaISy and the Abdominal and Direct Fetal Electrocardiogram Database, when no thoracic signals are available. The approach was tested on all three databases and a comparison was possible for one of the databases, namely the Abdominal and Direct Fetal Electrocardiogram Database, which contains a direct measurement in each dataset. With the approach it was possible to determine the fetal RR intervals with relatively good precision. Although some of the R peaks are missed during the processing of the abdominal signals, analyzing the signal for a longer interval can provide enough RR intervals for an accurate measurement of the fHR. A limitation for this approach could be the fact that it is mostly focused on the extraction of the fetal R-peaks only.

The comparison test showed that the combination of ICA and ANC can bring benefits in the extraction of the fECG from non-invasive measurements. Either with thoracic signals or without them, the combination of the mentioned blocks among with the other implemented blocks can lead to better performance than the individual methods. In the first approach this is due to the fact that the approach combines the contributions of both fetal signals (from ICA and from the ANC), allowing to give more priority to the variations that are common to both signals. In the second approach, the combination makes possible the use of the ANC in absence of thoracic signals that can be used as reference. The reference maternal signal is generated by ICA. Also, the combination made it possible to obtain a better fetal representation than the one obtained by ICA when tested on the Abdominal and Direct Fetal Electrocardiogram. Although the computation demand increases with the combined method, the fact that it brings the possibility of obtaining an fECG signal which the individual methods

cannot produce, justifies the raise of computation time and requirements.

4.2 Future Work

Following future work is considered:

- Design a system for removal of noise and artifacts (pre-processing) using advanced techniques such as Kalman filters, Wavelet transforms and LTV-filters. This for all common abdominal electrocardiogram noises such as powerline interference and high frequency noise and also for the common artifacts such as baseline wander and maternal activity such as uterus activity that may modify the quality of the abdominal signals.
- Implement an algorithm for the automatic identification of the fetal R peaks under high noise conditions for the analysis of the fetal heart rate variability.
- Make a comparison for the ANC block, using different optimization algorithms such as NLMS, RLS, etc. and establish an optimization algorithm for the length of the adaptive filter as well as for the rate of convergence.
- Build a database with both thoracic and abdominal signals, for different women, at different stages of pregnancy, using advanced acquisition equipment and analog techniques. The database should also contain parameters relative to the electrode position and, if possible, ecographies to determine the presentation of the fetus during each recording. Also, post-birth medical information would be important for exploring the relationship between the fECG and the post-birth health.

5 BIBLIOGRAPHY

- [1] R. Sameni and G. D. Clifford, "A Review of Fetal ECG Signal Processing; Issues and Promising Directions," *The Open Pacing, Electrophysiology and Therapy Journal*, vol. 3, pp. 4–20, 2010.
- [2] A. Khamene and S. Negahdaripour. "A New Method for the Extraction of Fetal ECG from the Composite Abdominal Signal," *IEEE Trans. on Biomed. Eng.*, vol. 47, no. 4, pp. 507 - 516, 2000.
- [3] D. Panigrahi, M. Rakshit and P. K. Sahu. "An Efficient Method for Fetal ECG Extraction From Single Channel Abdominal ECG," *Int. Conf. Ind. Instrum. Control. ICIC*, pp. 1083-1088, 2015.
- [4] S. Liu, D. Liu, J. Zhang and Y. Zeng. "Extraction of Fetal Electrocardiogram using Recursive Least Squares and Normalized Least Mean Squares Algorithms," *3rd Internat. Conf. on Advan. Comp. Control (ICACC)*, pp. 333 - 336, 2011.
- [5] V. Zarzoso, A. K. Nandi. "Noninvasive Fetal Electrocardiogram Extraction: Blind Separation Versus Adaptive Noise Cancellation," *IEEE Trans. on Biomed. Eng.*, vol. 48, no. 1, pp. 12 - 18, 2001.
- [6] N. Ivanushkina, K. Ivanko, E. Lysenko, I. Borovskiy and O. Panasiuk. "Fetal Electrocardiogram Extraction from Maternal Abdominal Signals," *XXXIV Internat. Scient. Conf. Electron. and Nanotech. (ELNANO)*, pp. 334 - 338, 2014.
- [7] V. Ionescu, M. Hnatiuc. "Fetal Heart Rate Detection and Monitoring From Noninvasive Abdominal ECG Recordings," *The 5th IEEE International Conference on E-Health and Bioengineering*, 2015.
- [8] J. Behar, F. Andreotti, J. Oster and G. D. Clifford. "A Bayesian Filtering Framework for Accurate Extracting of the Non-Invasive FECG Morphology," *Computing in Cardiology 2014*, pp. 53 - 56, 2014.
- [9] I. Silva, J. Behar, R. Sameni, T. Zhu, J. Oster, G. D. Clifford and G. B. Moody. "Noninvasive Fetal ECG: the PhysioNet/Computing in Cardiology Challenge 2013," *Computing in Cardiology 2013*, pp. 149 - 152, 2013.
- [10] L. Sörnmo and P. Laguna, "The Electrocardiogram - A Brief Background," in *Bioelectrical Signal Processing in Cardiac and Neurological Applications*, 1st ed., Burlington, USA: ELSEVIER Academic Press, pp. 411-452, 2005.
- [11] G. D. Clifford, F. Azuaje and P. McSharry, "The Physiological Basis of the Electrocardiogram," in *Advanced Methods And Tools for ECG Data Analysis*, 1st ed., Norwood, MA, USA: Artech House, pp. 1 - 25, 2006.
- [12] T. R. Barbeau. "Neuro-Physiology Supplements" [Online]. Available: http://people.fmarion.edu/tbarbeau/physio_neuro_supplements.htm. [Accessed: 22-Sept-2016]

- [13] A. C. Guyton and J. E. Hall. “Membrane Physiology, Nerve, and Muscle” in *Textbook of Medical Physiology*, 11th ed., Philadelphia, Pennsylvania: ELSEVIER SAUNDERS, 2006.
- [14] A. C. Guyton and J. E. Hall. “The Heart” in *Textbook of Medical Physiology*, 11th ed., Philadelphia, Pennsylvania: ELSEVIER SAUNDERS, 2006.
- [15] K. E. Barrett, S. M. Barman, S. Boitano and H. L. Brooks, “Origin of the Heartbeat & the Electrical Activity of the Heart,” in *Ganong’s Review of Medical Physiology*, 25th ed., New York, NY: McGraw-Hill, 2016.
- [16] A. Gacek and W. Pedrycz (editors). *ECG Signal Processing, Classification and Interpretation: A comprehensive Framework of Computational Intelligence*. 1st ed., New York: Springer, 2012.
- [17] E. M. Symonds, D. Sahota and A. Chang. *Fetal Electrocardiography*, 1st ed., London: Imperial College Press, 2001.
- [18] J. Behar, A. Johnson, G. D. Clifford and J. Oster, “A Comparison of Single Channel Fetal ECG Extraction Methods,” *Annals of Biomedical Engineering*, vol. 42, no. 6, pp. 1340 - 1353, 2014.
- [19] J. L. Semmlow. “Multivariate analyses: Principal Component Analysis and Independent Component Analysis,” in *Biosignal and Biomedical Image Processing*, 3rd ed., Boca Raton, FL: CRC Press, 2004.
- [20] G. D. Clifford. “Blind Source Separation: Principal & Independent Component Analysis,” *Biomedical Signal and Image Processing HST-582J/6.555J/16.456J*, MIT, (2008). [Online]. Available: http://www.mit.edu/~gari/teaching/6.555/LECTURE_NOTES/ch15_bss.pdf. [Accessed: 21-05-2017]
- [21] J. L. Semmlow. “Optimal and Adaptive Filters,” in *Biosignal and Biomedical Image Processing*, 3rd ed., Boca Raton, FL: CRC Press, 2004.
- [22] P. K. Partha, P. Sarbani and S. Goutam. “Fetal ECG Extraction from Single-Channel Maternal ECG Using Singular Value Decomposition,” *IEEE Trans. on Biomed. Eng.*, vol. 44, No 1, pp. 51-59, 1997.
- [23] M. Richter, T. Schreiber and D. T. Kaplan. “Fetal ECG Extraction with Nonlinear State-Space Projections,” *IEEE Trans. on Biomed. Eng.*, vol. 45, no. 1, pp. 133 - 137, 1998.
- [24] Y. Ye-Lin, G. Prats-Boluda, J. Alberola-Rubio, J. Garcia-Casado. “Combined method for fetal electrocardiogram extraction from non-invasive abdominal recordings,” *34th Annual Intern. Conf. of the IEEE EMBS*, pp. 356 - 359, 2012.
- [25] A. L. Goldberger, L. A. N. Amaral, L. Glass, J. M. Hausdorff, P. C. Ivanov, R. G. Mark, J. E. Mietus, G.B. Moody, C-K. Peng and H. E. Stanley. “PhysioBank, PhysioToolkit, and PhysioNet: Components of a New Research Resource for Complex Physiologic Signals”, *Circulation*, vol. 101, no. 23, pp. e215 - e220, Jun. 2000. [Online]. Available: <http://circ.ahajournals.org/content/101/23/e215.full>

- [26] M. Fatemi, M. Niknazar and R. Sameni. "A Robust Framework for Noninvasive Extraction of Fetal Electrocardiogram Signals," Computing in Cardiology 2013, pp. 201 - 204, 2013.
- [27] M. Nasiri, K. Faez and A. M. Nasrabadi. "A New Method for Extraction of Fetal Electrocardiogram Signal Based on Adaptive Nero-Fuzzy Inference System," IEEE Internat. Conf. on Signal and Image Proc. Appl., pp. 456 - 461, 2011.
- [28] M. Nasiri, K. Faez. "Extracting Fetal Electrocardiogram Signal Using ANFIS Trained by Genetic Algorithm," Internat. Conf. on Biomed. Eng. (ICoBE), pp. 197 - 202, 2012.
- [29] S. Lijuan, Z. Wei, G. Qun, L. Tiebing, L. Ping, T. Liming and L. Hongxing. "The fetal ECG data in DAISY database are from actual measuring?," 2011 Firs Intern. Workshop on Complexity and Data Mining, pp. 145 - 147, 2011.
- [30] A. A. Raoof K. Bsoul. "A Simple Noninvasive Approach for Fetal Electrocardiogram Extraction Based on Wavelet Transform," International Conf. on Advances in Biom. Eng. (ICABME), pp. 97 - 100, 2015.
- [31] W. K. Jenkins, H. Ding, M. Zenaldin, A. D. Salvia and R. M. Collins. "Adaptive Signal Processing Techniques for Extracting Fetal Electrocardiograms from Noninvasive Measurements," IEEE 57th Internat. Midwest Symp. on Circ. and Sys. (MWSCAS), pp. 639 - 642, 2014.
- [32] D. Shehada and A. H. Khandoker. "Non-Invasive Extraction of Fetal Electrocardiogram Using Fast Independent Component Analysis Technique," Middle East Conf. on Biomed. Eng. (MECBME), pp. 349 - 352, 2014.
- [33] B. D. Moor, P. D. Gersem, B. D. Schutter and W. Favoreel, "DAISY: A Database for Identification of Systems," Journal A, vol. 38, no. 3, pp. 4 - 5, 1997.
- [34] P. Husar. "Zeit-, Frequenz- und Verbundbereich" in *Biosignalverarbeitung*, 1st ed., Springer, 2010.
- [35] J. Pan and W. J. Tompkins. "A Real-Time QRS Detection Algorithm," IEEE Trans. on Biomed. Eng., vol. BME-32, no. 3, pp. 230 - 236, 1985.
- [36] Hyvärinen, Aapo, and Erkki Oja. "Independent Component Analysis: algorithms and applications," Neural networks 13.4 (2000): 411-430. [Online]. Available: <https://www.cs.helsinki.fi/u/ahyvarin/papers/NN00new.pdf>. [Accessed: 29-Apr-2017]
- [37] J-F. Cardoson and A. Souloumiac. "Blind Beamforming for Non-Gaussian Signals, " in IEE Proceedings-F, Vol. 140, No. 6, pp. 362 - 370, 1993.
- [38] J-F. Cardoso. "High-Order Contrasts for Independent Component Analysis," in Neural Computation 11, Massachusetts Institute of Technology, pp. 157 - 192, 1999.
- [39] P.E. McSharry, G.D. Clifford, L. Tarassenko L and L. Smith. "A dynamical model for generating synthetic electrocardiogram signals," IEEE Transactions on Biomedical Engineering 50(3), pp. 289-294, 2003.

- [40] J. Yen, D. Banks, P. Black, L. J. Gallagher, C. R. Hagwood, R. N. Kacker and L. S. Rosenthal. "Software Testing: Protocol Comparison," National Institute of Standards and Technology Gaithersburg, pp. 1 - 19, 1998. [Online]. Available: <http://www.itl.nist.gov/div897/ctg/stat/simulationmar98.pdf>. [Accessed: 25-Mar-2017]
- [41] D. E. Mohrman and L. J. Heller. "Overview of the Cardiovascular System," in *Cardiovascular Physiology*, 8th ed., New York, NY: McGraw-Hill, 2009.
- [42] J. G. Proakis and D. G. Manolakis. *Digital Signal Processing*, 4th ed., New Jersey, NJ: Pearson, 2006.
- [43] X. Yu, D. Hu and J. Xu . "Independent Component Analysis and Applications" in *Blind Source Separation, Theory and Applications*, 1st ed., Singapore: Wiley, 2014.